Oncogene (2014), 1–16

www.nature.com/onc

ORIGINAL ARTICLE

Targeting ErbB-2 nuclear localization and function inhibits breast cancer growth and overcomes trastuzumab resistance

RI Cordo Russo[1,4], W Béguelin[1,4], MC Díaz Flaqué[1], CJ Proietti[1], L Venturutti[1], N Galigniana[1], M Tkach[1], P Guzmán[2], JC Roa[2], NA O'Brien[3], EH Charreau[1], R Schillaci[1] and PV Elizalde[1]

Membrane overexpression of ErbB-2/HER2 receptor tyrosine kinase (membrane ErbB-2 (MErbB-2)) has a critical role in breast cancer (BC). We and others have also shown the role of nuclear ErbB-2 (NErbB-2) in BC, whose presence we identified as a poor prognostic factor in MErbB-2-positive tumors. Current anti-ErbB-2 therapies, as with the antibody trastuzumab (Ttzm), target only MErbB-2. Here, we found that blockade of NErbB-2 action abrogates growth of BC cells, sensitive and resistant to Ttzm, in a scenario in which ErbB-2, ErbB-3 and Akt are phosphorylated, and ErbB-2/ErbB-3 dimers are formed. Also, inhibition of NErbB-2 presence suppresses growth of a preclinical BC model resistant to Ttzm. We showed that at the cyclin D1 promoter, ErbB-2 assembles a transcriptional complex with Stat3 (signal transducer and activator of transcription 3) and ErbB-3, another member of the ErbB family, which reveals the first nuclear function of ErbB-2/ErbB-3 dimer. We identified NErbB-2 as the major proliferation driver in Ttzm-resistant BC, and demonstrated that Ttzm inability to disrupt the Stat3/ErbB-2/ErbB-3 complex underlies its failure to inhibit growth. Furthermore, our results in the clinic revealed that nuclear interaction between ErbB-2 and Stat3 correlates with poor overall survival in primary breast tumors. Our findings challenge the paradigm of anti-ErbB-2 drug design and highlight NErbB-2 as a novel target to overcome Ttzm resistance.

Oncogene advance online publication, 1 September 2014; doi:10.1038/onc.2014.272

INTRODUCTION

ErbB-2, a member of the ErbB family of receptor tyrosine (Tyr) kinases (EGF-R/ErbB-1, ErbB-2, ErbB-3 and ErbB-4), is a major player in the breast cancer (BC) scenario. Membrane ErbB-2 (MErbB-2) overexpression or gene amplification in human BC are associated with increased metastatic potential and poor prognosis.[1–3] ErbB ligands include all isoforms of heregulins (HRGs), which bind to ErbB-3 and ErbB-4, and recognize EGF-R and ErbB-2 as coreceptors.[4] Upon HRG binding, ErbBs form homo- and heterodimers. This stimulates their Tyr kinase activity and results in the activation of signaling pathways, the classic transduction mechanism of ErbB's proliferative effects. Although ErbB-2 is an orphan receptor, it dimerizes with the other ErbBs. In BC cells overexpressing MErbB-2, it also assembles homo- and heterodimers in the absence of ligand.[5,6] Membrane ErbB-3 (MErbB-3) critical role as ErbB-2 coreceptor mediating ligand-independent and HRG-induced ErbB-2 signaling and growth effects in BC has been proved in several works, including ours.[7–13] Also, MErbB-3 overexpression is a prognosis of poor BC survival.[14,15]

Current therapeutic options for patients whose tumors overexpress MErbB-2 (ErbB-2-positive BC subtype) include monoclonal antibodies (trastuzumab (Ttzm) and pertuzumab), Tyr kinase inhibitors (lapatinib) and trastuzumab-DM1, an antibody–drug conjugate. Despite a significant clinical response to Ttzm, the first anti-ErbB-2 therapy approved for metastatic and early-stage BC,[16,17] around 40 to 60% of patients with MErbB-2-overexpressing metastatic BC do not respond to Ttzm, showing either *de novo* or acquired resistance.[16,18]

A major contribution to the understanding of the ErbB-2 biology was the demonstration that MErbB-2 migrates to the nucleus (nuclear ErbB-2 (NErbB-2)), where it acts as a transcription factor.[19] We showed that in BC cells stimulated with progestin, ErbB-2 assembles a transcriptional complex in which it functions as a coactivator of the signal transducer and activator of transcription 3 (Stat3), another key regulator in BC, to promote the expression of cyclin D1 and induce growth.[20] The nuclear presence of several HRG isoforms as well as of ErbB-3 was detected in BC cells and primary tumors.[6,21–24] However, HRG and ErbB-3 nuclear function in BC remains poorly known.

Here, we explored basal and HRG-modulated nuclear interaction and function of ErbB-2 and ErbB-3 and their role in proliferation and response to Ttzm in ErbB-2-positive BC. We revealed the first nuclear function of the ErbB-2/ErbB-3 dimer. Our findings showed that NErbB-2 is the major driver of growth in Ttzm-resistant BC, and demonstrated that blockade of NErbB-2 localization is a novel therapeutic strategy to overcome Ttzm resistance.

RESULTS

Nuclear ErbB-2 drives HRGβ1-induced BC growth

We previously found that inhibition of NErbB-2 presence blocks progestin-induced growth of the ErbB-2- and ErbB-3-overexpressing C4HD murine BC model.[20] To block NErbB-2

[1]Laboratory of Molecular Mechanisms of Carcinogenesis, Instituto de Biología y Medicina Experimental (IBYME), CONICET, Buenos Aires, Argentina; [2]Departamento de Anatomía Patológica (BIOREN), Universidad de La Frontera, Temuco, Chile and [3]Department of Medicine, Division of Hematology/Oncology, Geffen School of Medicine at UCLA, Los Angeles, CA, USA. Correspondence: Dr PV Elizalde, Laboratory of Molecular Mechanisms of Carcinogenesis, Instituto de Biología y Medicina Experimental (IBYME), CONICET, Obligado 2490, Buenos Aires 1428, Argentina.
E-mail: patriciaelizalde@ibyme.conicet.gov.ar
[4]These authors contributed equally to this work.
Received 12 May 2014; revised 8 July 2014; accepted 19 July 2014

presence, we transfected cells with a human ErbB-2 nuclear localization domain mutant (hErbB-2ΔNLS), unable to translocate to the nucleus,[25] and which functions as a dominant-negative (DN) inhibitor of endogenous ErbB-2 nuclear migration.[20] Here, we found that HRGβ1 induced ErbB-2 nuclear localization in C4HD cells (Supplementary Figure S1a). hErbB-2ΔNLS acts as DN inhibitor of endogenous ErbB-2 nuclear translocation, retains its intrinsic Tyr kinase activity and functions as an upstream activator of Stat3 phosphorylation in C4HD cells treated with HRGβ1 (Supplementary Figures S1b and c). ErbB-2 silencing abrogated HRGβ1 proliferative effects, which were restored when we re-expressed wild-type human ErbB-2 (ErbB-2-WT), but not hErbB-2ΔNLS (Figure 1a). Transfection of hErbB-2-ΔNLS into cells retaining their endogenous ErbB-2 abrogated the proliferative response to HRGβ1 (Figure 1a and Supplementary Figure S1d), consistent with our findings that hErbB-2-ΔNLS is a DN inhibitor of endogenous ErbB-2 proliferative effects in BC.[20] Proliferation of C4HD cells under basal conditions, in which ErbB-2 is not present at the nucleus,[20] was not affected by transfection with hErbB-2ΔNLS. Next, we developed an *in vivo* BC model induced by HRGβ1. C4HD cells transfected with the empty pcDNA3.1 vector (C4HD) were inoculated subcutaneously into nude mice implanted with HRGβ1 pellets. While all mice receiving HRGβ1 developed tumors, no tumors arose in the control group implanted with bovine serum albumin pellets (Figures 1b and c). Tumors from mice receiving HRGβ1 were grade III carcinomas with an invasive growth pattern and with lack of glandular or tubular differentiation (Figure 1b). We also conducted a preclinical study of inhibition of NErbB-2 presence in this model. Cells transfected with the hErbB-2ΔNLS (C4HD-hErbB-2ΔNLS) were inoculated into mice implanted with the HRGβ1 pellets. Only three out of six mice injected with C4HD-hErbB-2ΔNLS cells developed tumors. Mean volume and growth rates of C4HD-hErbB-2ΔNLS tumors were significantly lower than those of C4HD (Figures 1b and c). C4HD-hErbB-2ΔNLS tumors showed lower histologic grade (II) as compared with C4HD, their growth pattern was less invasive and they display glandular differentiation (Figure 1b). Consistent with our previous *in vitro* findings with HRGβ1,[9,11,12] in C4HD tumors we observed ErbB-2 phosphorylation at Tyr 1272 (Tyr 1222 in the human protein), an autophosphorylation site, and at Tyr 927 (Tyr 877 in human), a site different from the autophosphorylation ones and whose phosphorylation we previously detected in NErbB-2.[20] Here, we also found ErbB-3 and Stat3 phosphorylation in C4HD tumors (Figure 1d). Increased phosphatidylinositol 3-kinase (PI3K)/AKT pathway activation[26,27] and presence of HRGβ1-induced MErbB-2/ErbB-3 dimers[28,29] have been found to cause Ttzm resistance. Interestingly, we detected the same levels of ErbB-2, ErbB-3, Stat3 and Akt phosphorylation, and of ErbB-2/ErbB-3 dimers, in C4HD-hErbB-2ΔNLS and C4HD tumors (Figures 1d and e). At the end of the experiment, ~36% of the cells still expressed the green fluorescent protein (GFP)-tagged hErbB-2ΔNLS mutant (Supplementary Figure S1e). These findings demonstrate that blockade of ErbB-2 nuclear localization inhibits *in vivo* growth of MErbB-2-positive BC in a scenario where HRGβ1 induces ErbB-2 and ErbB-3 phosphorylation and heterodimerization and where Akt is highly phosphorylated.

Comparison between hErbB-2ΔNLS and Ttzm effects in ErbB activation and BC growth

NErbB-2 was already detected in MErbB-2-overexpressing and Ttzm-sensitive BT-474 and SK-BR-3 cells.[19,30–32] Here, we found that HRGβ1 further stimulated ErbB-2 nuclear migration, which remained unaffected by Ttzm (Figure 2a). While basal MErbB-2 levels were significantly higher than those of NErbB-2 in both cell lines, HRGβ1 treatment inverted the ratio of NErbB-2 to MErbB-2 in SK-BR-3 cells, and increased the levels of NErbB-2 in BT-474 by 80% (Figures 2a and b). Transfection with hErbB-2ΔNLS abrogated basal and HRGβ1-induced ErbB-2 nuclear translocation (Figure 2c). Also, hErbB-2ΔNLS induced comparable levels of basal growth inhibition to those exerted by Ttzm (Figure 2d). The addition of exogenous ErbB ligands was found to overcome Ttzm antiproliferative effects.[31,33,34] Contrastingly, the antiproliferative effects of hErbB-2ΔNLS were not counteracted by HRGβ1 (Figure 2d). Constitutive ErbB-2 phosphorylation at Tyr 1222 and Tyr 877 was found in both lines, which was significantly decreased by HRGβ1 (Figure 2e), as described for Tyr 877.[29,31] Ttzm has already been found to decrease,[35] increase[27,30,31] or have no effect on ErbB-2 phosphorylation in BC.[29] Here, we found that it significantly stimulates ErbB-2 phosphorylation, which was not modified by its combination with HRGβ1 (Figure 2e). Transfection with hErbB--2ΔNLS did not modify ErbB-2 basal phosphorylation or ErbB-2 phosphorylation induced by HRGβ1 (Figure 2e). It is well acknowledged that HRGβ1 stimulates ErbB-3 phosphorylation, leading to Akt activation in BC cells,[36,37] an effect that is not counteracted by Ttzm.[29,33] Our present findings showed that HRGβ1 effects on ErbB-3 phosphorylation and Akt activation also remained unaffected by transfection with hErbB-2ΔNLS (Figure 2e). Like in previous findings in HRG-stimulated and Ttzm-treated cells,[29] ErbB-2/ErbB-3 heterodimers were detected in hErbB-2ΔNLS-transfected cells treated with HRGβ1 (Figure 2f). These findings are in accordance with our *in vivo* results in the mouse model and reveal that inhibition of NErbB-2 presence abolishes growth of MErbB-2-overexpressing human BC cells, in spite of HRGβ1-induced formation of ErbB-2/ErbB-3 dimers leading to ErbB-3 phosphorylation and PI3K/AKT pathway activation. Contrastingly, Ttzm is not capable of abrogating proliferation of either BC cells with increased PI3K/AKT activation or which display ErbB-2/ErbB-3 dimers formed upon HRGβ1 stimulation.[27,29,34,38]

Inhibition of ErbB-2 nuclear localization blocks proliferation in Ttzm-resistant BC

We examined hErbB-2ΔNLS effects on the proliferation of intrinsically Ttzm-resistant JIMT-1 human BC cells.[39] JIMT-1 cells show several molecular traits underlying Ttzm resistance, such as an activating mutation in *PIK3CA*, the gene that codes for the p110α catalytic subunit of PI3K, low levels of PTEN and high content of HRG.[40,41] NErbB-2 was readily detected in JIMT-1 cells. Its levels were significantly higher than those of MErbB-2 and were enhanced by HRGβ1 (Figures 3a and b). Ttzm did not modify basal levels of NErbB-2 and was unable to inhibit HRGβ1-induced ErbB-2 nuclear migration (Figure 3a and Supplementary Figure S2a, which shows quantification of confocal images). On the contrary, transfection with hErbB-2ΔNLS blocked ErbB-2 nuclear localization in HRGβ1-treated and -untreated cells (Figure 3a). ErbB-2-amplified and intrinsic Ttzm-resistant MDA-MB-453 and HCC1569 cells also display basal ratios of MErbB-2/NErbB-2 lower than 1 (Figure 3b displays the quantification of confocal images shown in Supplementary Figure S2b). As reported,[41] MErbB-2 levels in JIMT-1, MDA-MB-453 and HCC1569 cells were significantly lower than those in Ttzm-sensitive BT-474 and SK-BR-3 cells (Figure 3c, confocal images shown in Figure 2a and Supplementary Figure S2b). Ttzm-resistant HCC1419 cells showed a ratio of MErbB-2/NErbB-2 higher than 1. However, their basal NErbB-2 expression was significantly higher than in responsive cells (Figure 3d displays the quantification of confocal images shown in Supplementary Figure S2b). Acquisition of Ttzm resistance in BT-474 clones does not involve changes in MErbB-2 levels,[41,42] nor in total Stat3 expression (Supplementary Figure S2c). Here, we found the same result in a BT-474HR clone we selected for its acquired resistance to Ttzm[42] (Figure 3c, and images in Supplementary Figure S2b), where, however, we found increased NErbB-2 levels, and consequently decreased MErbB-2/NErbB-2 ratios as compared with parental cells (Figures 3b, d and 2b). HRGβ1 increased NErbB-2 levels in all Ttzm-resistant cells (Figure 3d and

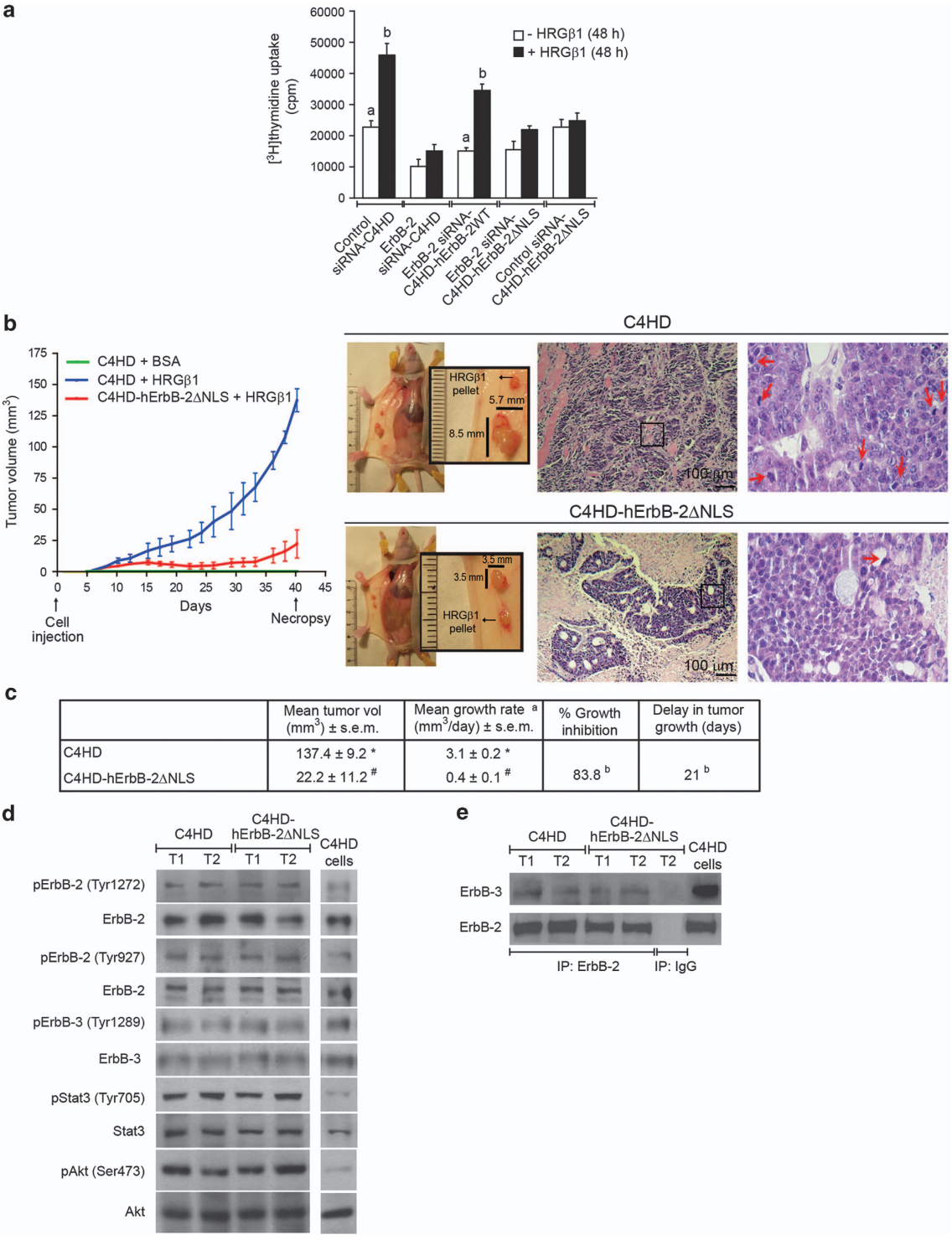

	Mean tumor vol (mm^3) ± s.e.m.	Mean growth rate [a] (mm^3/day) ± s.e.m.	% Growth inhibition	Delay in tumor growth (days)
C4HD	137.4 ± 9.2 *	3.1 ± 0.2 *		
C4HD-hErbB-2ΔNLS	22.2 ± 11.2 #	0.4 ± 0.1 #	83.8 [b]	21 [b]

Figure 1. Nuclear ErbB-2 drives HRGβ1-induced BC growth. (**a**) Endogenous ErbB-2 expression was silenced by transfection with ErbB-2 siRNAs and expressions of either hErbB-2WT or hErbB-2ΔNLS were restored by co-transfection with the respective plasmids. Cells were treated with HRGβ1 and [^{3}H]thymidine incorporation was used as a measure of DNA synthesis. Data are presented as mean ± s.d. For b vs a: $P < 0.001$. The experiment shown is representative of a total of three. (**b**) Preclinical model of *in vivo* blockade of ErbB-2 nuclear localization. Left panel: Cells (10^6) were inoculated subcutaneously in mice treated with HRGβ1. As control, mice were injected with pcDNA3.1 vector-transfected cells (C4HD) and treated with bovine serum albumin (BSA). Each point represents the mean tumor volume ± s.e.m. Right panel: Decrease in tumor mass and histopathologic analysis of tumors. Hematoxylin and eosin (H&E) staining of histologic sections from tumors excised at day 40. Mitoses are indicated with red arrows. (**c**) Tumor growth. [a]Growth rates were calculated as the slopes of growth curves. Volume, percentage of growth inhibition and delay in tumor growth were calculated at day 40. # vs *: $P < 0.001$. [b]With respect to C4HD cells, $P < 0.001$. (**d**) Tumor lysates were analyzed by WB. Shown are two representative tumors from each group. C4HD cells not treated with HRGβ1 were used as a control for the protein phosphorylation state. (**e**) Tumor lysates were immunoprecipitated (IP) with ErbB-2 and analyzed by WB with ErbB-3 antibodies. Membranes were reprobed with ErbB-2 antibodies. IgG was used as control of specificity. Total lysates from C4HD cells transfected with the empty pcDNA3.1 vector were blotted in parallel (see Supplementary Figure S1).

Supplementary Figure S2b). Transfection of hErbB-2ΔNLS inhibited JIMT-1 cell growth, which was not affected by HRGβ1 (Figure 3e). This blockade of proliferation occurs in a scenario in which ErbB-2, ErbB-3 and Akt are phosphorylated, and ErbB-2/ErbB-3 dimers are formed in both HRGβ1-treated and -nontreated cells (Figures 3f and g). hErbB-2ΔNLS also functioned as a DN inhibitor of endogenous ErbB-2 nuclear migration in a panel of Ttzm-resistant lines (Supplementary Figure S2d), and inhibited basal and HRGβ1-stimulated growth of these lines (Figure 3h). Next, we developed a preclinical model where JIMT-1 cells were transfected

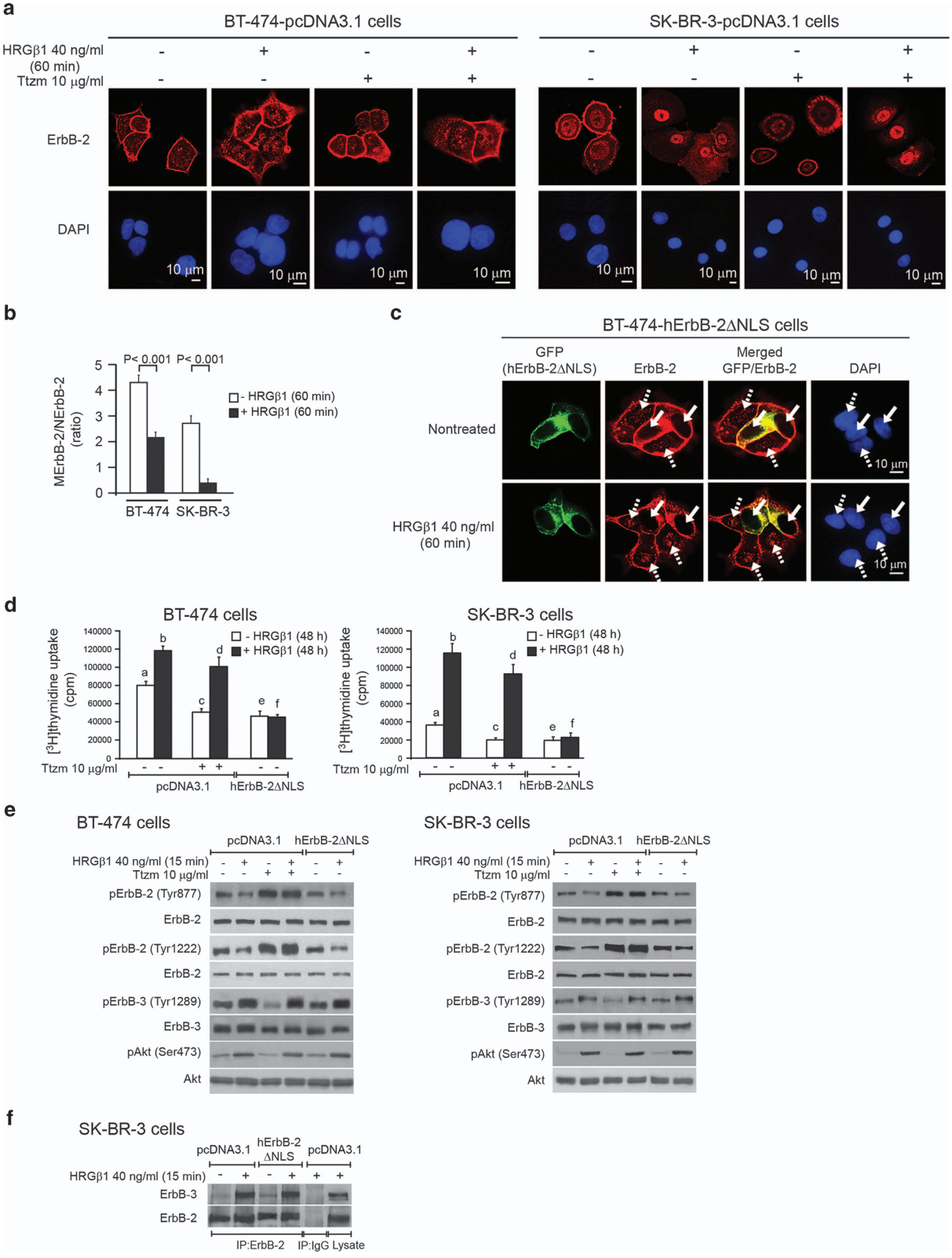

with hErbB-2ΔNLS (JIMT-1-hErbB-2ΔNLS) or pcDNA3.1 (JIMT-1) and were inoculated into nude mice. When JIMT-1 tumors reached 40 mm^3, mice were divided into three groups and injected with Ttzm or immunoglobulin G (IgG), or remained untreated. Only two out of eight mice injected with JIMT-1-hErbB-2ΔNLS cells developed tumors. Mean volume and growth rates of JIMT-1-hErbB-2ΔNLS tumors were significantly lower than those of JIMT-1 (Figures 3i and j). As reported previously,[43,44] no significant differences were observed either in mean volumes or growth rates between tumors developed from JIMT-1 cells and those from JIMT-1 cells treated with Ttzm (Figures 3i and j). Our results reveal that abrogation of NErbB-2 presence is a successful strategy to block proliferation in Ttzm-resistant BC.

ErbB-2, ErbB-3, Stat3 and HRGβ1 colocalize and physically associate in the nucleus

We used BC cells devoid of basal NErbB-2 as the simplest model to explore the mechanism underlying NErbB-2 action and focused on the nuclear interaction between Stat3 and ErbB-2 we previously identified.[20] As found in C4HD cells (Figures 4a and b and Supplementary Figure S1), HRGβ1 caused ErbB-2 nuclear translocation in T47D human BC cells (Figures 4a and b). Full-length ErbB-2 nuclear translocation was shown by the identical molecular mass of NErbB-2 compared with that of ErbB-2 in total cell extracts, corresponding to the entire 185 kDa protein (Figure 4a) and was also shown by our findings with both the ErbB-2 carboxyl- and amino-terminal antibodies. Comparable also with our results in C4HD cells (Figure 1a and Supplementary Figure S1d), blockade of HRGβ1-induced NErbB-2 presence inhibited HRGβ1-stimulated but not basal T47D cell growth (Supplementary Figure S3a). Taken together, our findings in C4HD cells overexpressing MErbB-2 and in T47D cells displaying moderate amounts of MErbB-2 confirm the specificity of hErbB-2ΔNLS action, which abrogates BC cell proliferation only when driven by NErbB-2. Inhibition of HRGβ1-induced ErbB-2 phosphorylation with the kinase inhibitor AG825 (Supplementary Figure S3b) blocked ErbB-2 nuclear migration (Figures 4a and b). HRGβ1 also stimulated Stat3 nuclear translocation (Figures 4a and b). Stat3 tyrosine phosphorylation is mandatory for its nuclear migration.[45,46] Consistently, preincubation with AG825, which we found prevents HRGβ1/ErbB-2-stimulated Stat3 phosphorylation,[11] abolished Stat3 nuclear localization (Figures 4a and b). HRGβ1 stimulated nuclear colocalization and physical association of ErbB-2 with Stat3 (Figures 4b and c). HRGβ1 also caused ErbB-3 nuclear migration, where it is phosphorylated at Tyr 1289 (Figures 4a and d). Inhibition of ErbB-2 phosphorylation with AG825, which abrogates ErbB-2-mediated ErbB-3 tyrosine phosphorylation,[8,47] prevented ErbB-3 nuclear translocation, revealing that ErbB-3 phosphorylation is required for its nuclear migration (Figure 4a). ErbB-3 colocalizes with ErbB-2 at the membrane in the absence of HRGβ1 (Figure 4d). Here we found that HRGβ1 induces nuclear colocalization of ErbB-2 and ErbB-3 (Figure 4d). HRGβ1 itself translocates to the nucleus where it colocalizes with ErbB-2 (Figure 4e). We also found physical association among ErbB-2, ErbB-3 and HRGβ1 in the nucleus, and between Stat3 and ErbB-3 (Figure 4f). These findings reveal that HRGβ1 induces the formation of nuclear ErbB-2/ErbB-3 dimers, to which HRGβ1 remains bound, and which assemble a multimeric protein complex with Stat3 in BC cells. Basal nuclear Stat3 (NStat3) and ErbB-3 (NErbB-3), as well as ErbB-2/Stat3 and ErbB-2/ErbB-3 colocalization, were found in BT-474 and JIMT-1 cells (Figures 4g and h), where HRGβ1 further stimulated migration and colocalization of said proteins. Basal levels of NStat3 and NErbB-3 and their colocalization with NErbB-2 were significantly higher in JIMT-1 than in BT-474 cells (Figures 4g and h). Contrastingly, the majority of ErbB-2/ErbB-3 dimers were localized at the cytoplasmic membrane in BT-474 cells (Figure 4h). Our studies of hErbB-2ΔNLS actions showed that it colocalized with ErbB-3 at the membrane and at the cytoplasm, and abrogated HRGβ1-induced ErbB-3 nuclear translocation (Figure 4i). Ttzm failed to block basal and HRGβ1-induced ErbB-2 and Stat3 nuclear translocation, and consequently ErbB-2/Stat3 nuclear colocalization in BT-474 and JIMT-1 cells (Supplementary Figure S3c).

HRGβ1 induces the assembly of a Stat3/ErbB-2/ErbB-3 transcriptional complex at the cyclin D1 promoter in both Ttzm-sensitive and -resistant BC cells

We previously found that in BC, progestin induces the assembly of a Stat3/ErbB-2 transcriptional complex at the Stat3-response elements (GAS) of the cyclin D1 promoter, where ErbB-2 acts as a Stat3 coativator.[20] The proximal 1-kb cyclin D1 promoter lacks ErbB-2 binding sites (HER2-associated sequences, HAS). Here, we found that HRGβ1 induced cyclin D1 protein and mRNA expressions in BC cells (Figures 5a and b and Supplementary Figure S4a). Inhibition of ErbB-2 (AG825) and Stat3 (Jak inhibitor I, Proietti *et al.*[11]) activity or knockdown of their expressions abrogated HRGβ1 effects (Figures 5b and c and Supplementary Figure S4b). These findings identify Stat3 as a novel player in HRGβ1 modulation of cyclin D1 expression in BC. Chromatin immunoprecipitation (ChIP) and sequential ChIP assays in C4HD and T47D cells using primers spanning GAS sites in the mouse and human cyclin D1 promoters, respectively, showed that HRGβ1 induces Stat3, ErbB-2 and ErbB-3 simultaneous binding to the said region (Figures 5d and e). These findings identify the first nuclear function of the ErbB-2/ErbB-3 dimer recruited along with Stat3 at the GAS sites of the cyclin D1 promoter. This transcriptional complex was also assembled under basal and HRGβ1-induced conditions in BT-474 and JIMT-1 cells. Basal levels of corecruitment of all three proteins were higher in JIMT-1 cells than in BT-474 (Figure 5f). Figure 5g shows HRGβ1 stimulation of cyclin D1 protein expression.

Figure 2. Comparison between hErbB-2ΔNLS and Ttzm effects in ErbB activation and BC growth. (**a**) Cells were transfected with the empty pcDNA3.1 vector and treated with HRGβ1, Ttzm or pretreated with Ttzm before HRGβ1 stimulation. ErbB-2 (red) was localized by IF and confocal microscopy. Nuclei were stained with 4′,6-diamidino-2-phenylindole (DAPI) (blue). (**b**) Quantitative analysis of ErbB-2 subcellular localization in confocal images of cells treated or untreated with HRGβ1 from panel (**a**). Fluorescence intensity ratio of MErbB-2 vs NErbB-2 was calculated for 50 cells from each group. Data are presented as mean ± s.d. (**c**) Effect of hErbB-2ΔNLS on ErbB-2 nuclear migration. BT-474 cells were transfected with hErbB-2ΔNLS and treated with HRGβ1 or remained untreated. GFP from hErbB-2ΔNLS vector was visualized by direct fluorescence imaging (green), and total ErbB-2 (red) was localized by IF. Solid arrows: Cells transfected with hErbB-2ΔNLS; dashed arrows: wild-type cells that did not uptake the hErbB-2ΔNLS mutant. Nuclei were stained with DAPI (blue). (**d**) Inhibition of ErbB-2 nuclear localization abolishes basal and HRGβ1-induced *in vitro* proliferation. Cells were transfected with hErbB-2ΔNLS or pcDNA3.1 vector. When indicated, cells were pretreated with Ttzm and were then treated with HRGβ1 or remained untreated. Incorporation of [^{3}H]thymidine was used as a measure of DNA synthesis. Data are presented as mean ± s.d. For c and e vs a: $P < 0.01$; b vs a, d vs c and f vs b and d: $P < 0.001$. (**e**) Effects of hErbB-2ΔNLS on ErbB signaling. Cells were transfected as in (**d**) and were treated with HRGβ1, or were pretreated with Ttzm before HRGβ1 stimulation. WB analyses were performed with the indicated phospho (p) antibodies, and filters were reprobed with the respective total antibody. (**f**) Protein extracts from SK-BR-3 cells were immunoprecipitated (IP) with ErbB-2 and analyzed by WB with ErbB-3 antibodies. As control for the specificity of the protein interaction, lysates were IP with rabbit IgG. Total cell lysates were blotted in parallel. The experiments shown in (**a–f**) are representative of a total of three.

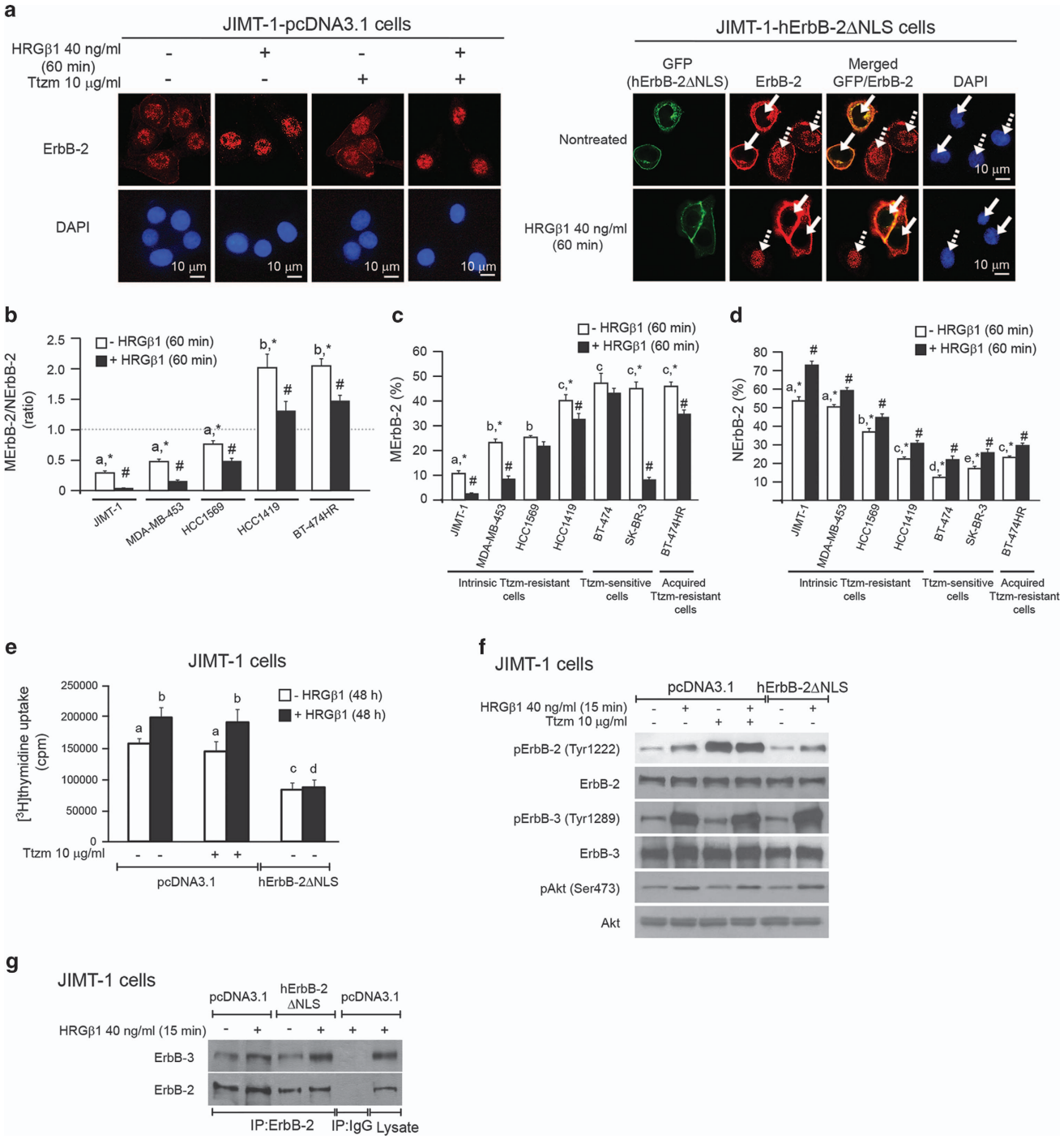

Figure 3. Inhibition of ErbB-2 nuclear localization blocks proliferation in Ttzm-resistant BC. (**a**) Cells transfected with pcDNA3.1 (left) or hErbB-2ΔNLS (right) vectors were treated as indicated. ErbB-2 (red) and GFP-tagged-hErbB-2ΔNLS (green) were localized as in Figure 2. Solid arrows: hErbB-2ΔNLS-transfected cells; dashed arrows: wild-type cells that did not uptake the hErbB-2ΔNLS mutant. Nuclei were stained with 4′,6-diamidino-2-phenylindole (DAPI) (blue). (**b–d**) Quantitative analysis of ErbB-2 subcellular localization. Fluorescence intensities of MErbB-2 and NErbB-2 were quantified in 50 cells from each group and are plotted as the ratio of MErbB-2/NErbB-2 (**b**), the percentage of MErbB-2 (**c**) or the percentage of NErbB-2 (**d**) (mean ± s.d.). For # vs *: $P < 0.001$. For b–e vs a, c–e vs b, and d vs c: $P < 0.001$. For c and d vs e: $P < 0.05$. (**e**) Blockade of NErbB-2 localization inhibits *in vitro* growth. Cells were transfected and treated as indicated. Proliferation and data were analyzed as in Figure 2. For b and c vs a, and d vs b: $P < 0.001$. (**f** and **g**) Effect of hErbB-2ΔNLS on ErbB signaling. Cells were transfected and treated as in (**e**). WB analysis (**f**) and immunoprecipitation analysis (**g**) were performed as in Figure 2. (**h**) Cell proliferation in intrinsic and acquired Ttzm-resistant cells was evaluated by [^{3}H]thymidine incorporation or cell count. Data are presented as in (**e**). For b and c vs a, and d vs b: $P < 0.001$. Experiments in (**a–h**) were repeated three times, with similar results. (**i**) hErbB-2ΔNLS blocks *in vivo* growth. Left panel: Cells were inoculated subcutaneously in mice. When JIMT-1 tumors reached 40 mm^3, animals were divided into three groups and injected with Ttzm, IgG or remained untreated. JIMT-1-hErbB-2ΔNLS-injected mice developed tumors with a latency of 40 days. Each point represents the mean tumor volume ± s.e.m. Right panel: Decrease in tumor mass. (**j**) Tumor growth. [a]Growth rates were calculated as in Figure 1. Volume, percentage of growth inhibition and delay in tumor growth from the different groups with respect to tumors from JIMT-1 cells were calculated at day 64. # vs *: $P < 0.001$. [b]With respect to JIMT-1 cells, $P < 0.001$ (see Supplementary Figure S2).

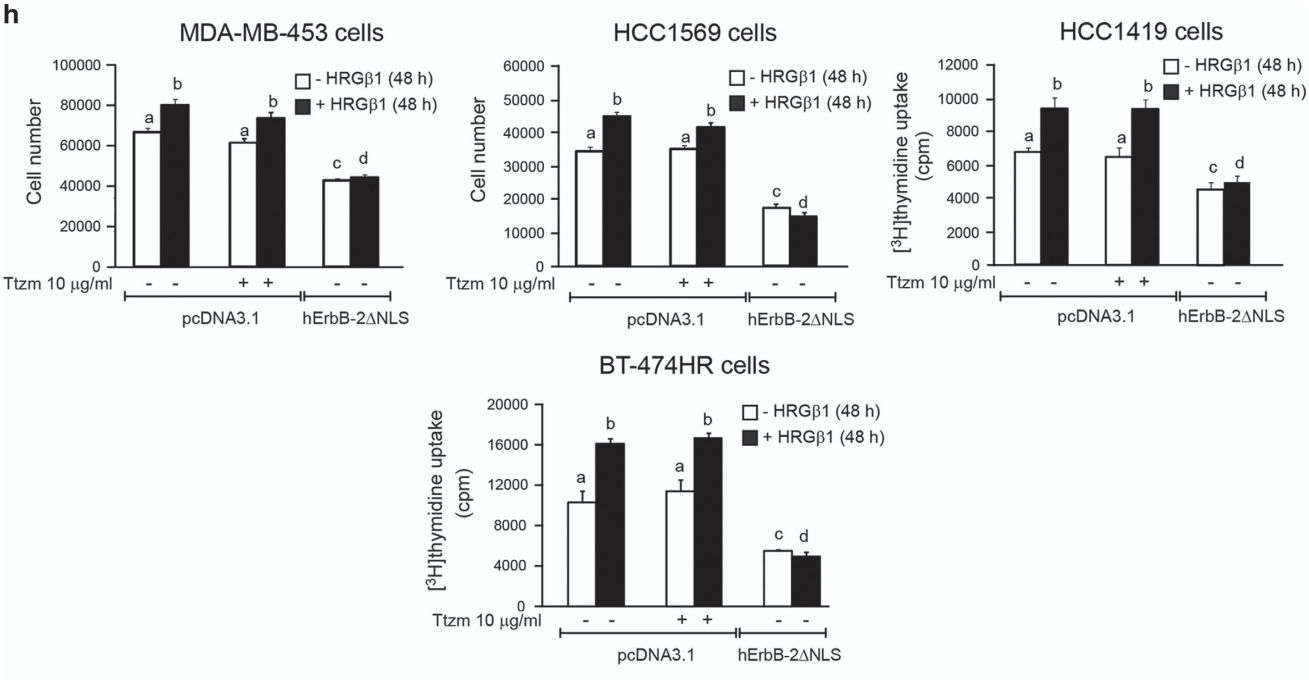

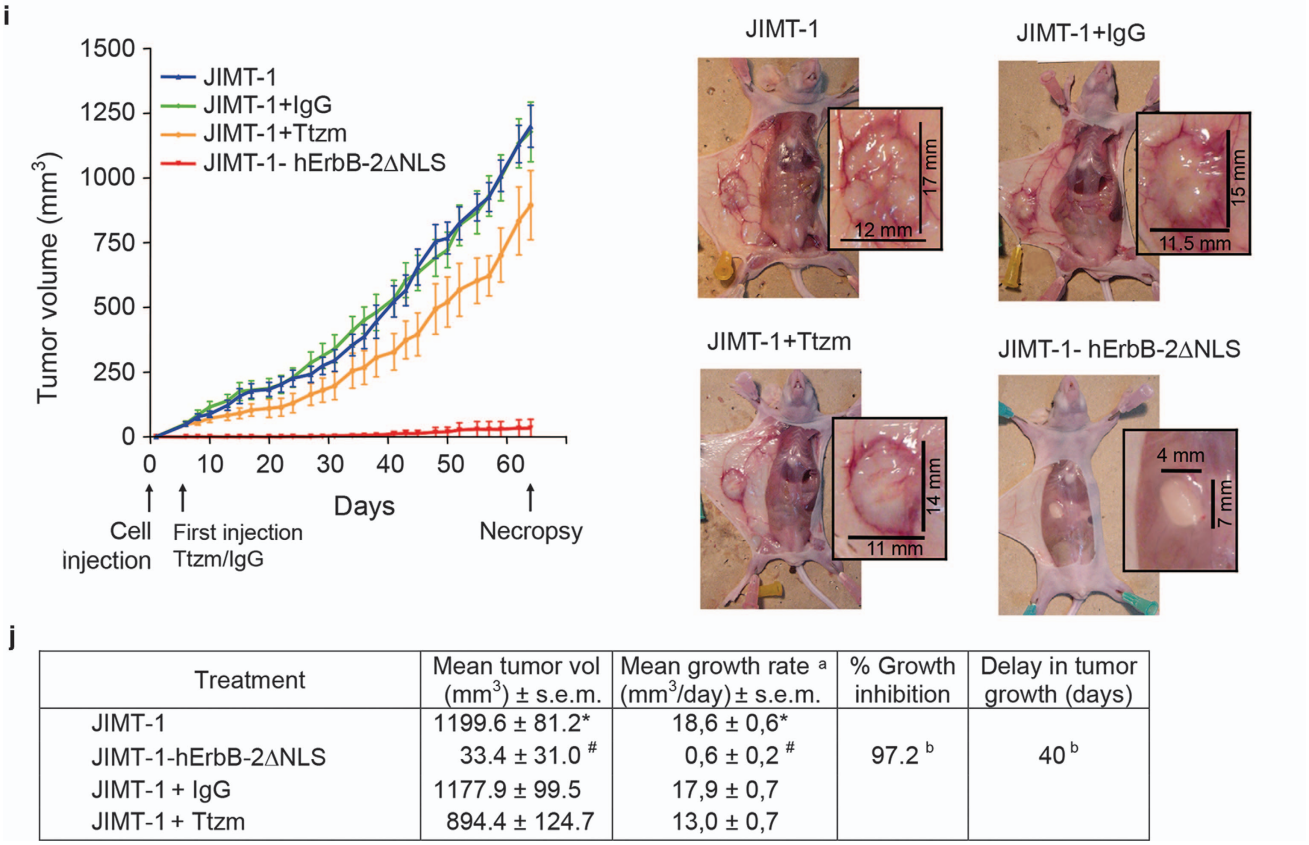

j

Treatment	Mean tumor vol (mm^3) ± s.e.m.	Mean growth rate [a] (mm^3/day) ± s.e.m.	% Growth inhibition	Delay in tumor growth (days)
JIMT-1	1199.6 ± 81.2*	18,6 ± 0,6*		
JIMT-1-hErbB-2ΔNLS	33.4 ± 31.0 #	0,6 ± 0,2 #	97.2 [b]	40 [b]
JIMT-1 + IgG	1177.9 ± 99.5	17,9 ± 0,7		
JIMT-1 + Ttzm	894.4 ± 124.7	13,0 ± 0,7		

Figure 3. Continued.

Disruption of the Stat3/ErbB-2/ErbB-3 nuclear complex is the differential molecular signature underlying hErbB-2ΔNLS growth inhibitory effects in Ttzm-resistant cells

As we found that the signaling activated after Ttzm treatment of JIMT-1 cells was the same as after transfection with the hErbB-2ΔNLS (Figures 3f and g), we compared Ttzm and hErbB-2ΔNLS effects on the assembly of the Stat3/ErbB-2/ErbB-3 nuclear complex. Ttzm was unable to block basal and HRGβ1-induced ErbB-2 and ErbB-3 recruitment to the GAS sites at the cyclin D1 promoter (Figure 6a). Contrastingly, ErbB-2 was not recruited to this site in cells transfected with the hErbB-2ΔNLS in basal or HRGβ1-stimulated conditions (Figure 6a), because of its function as DN inhibitor of endogenous ErbB-2 nuclear localization. In the absence of ErbB-2 recruitment, neither was ErbB-3 loaded at

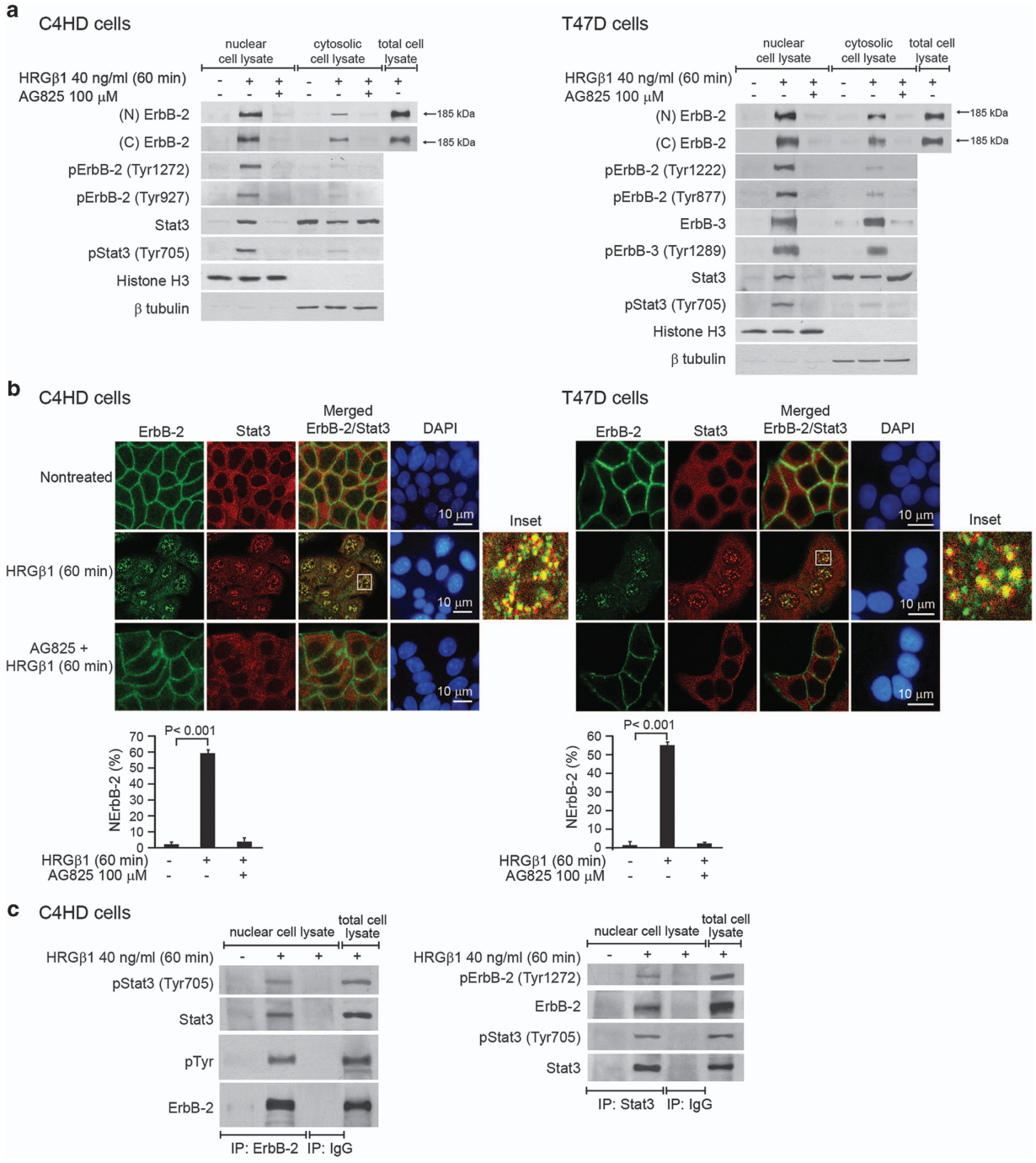

Figure 4. ErbB-2, ErbB-3, Stat3 and HRGβ1 colocalize and physically associate in the nucleus. (**a**) HRGβ1 induces ErbB-2, ErbB-3 and Stat3 nuclear migration. Cells were treated as indicated. Nuclear and cytosolic protein extracts were analyzed by WB with phospho (p) antibodies and reprobed with total antibodies. pErbB-2 blots were reprobed with ErbB-2 carboxyl (C)- or amino (N)-terminal antibodies as indicated. For ErbB-2, total lysates were blotted. Histone H3 and β-tubulin were used to control cellular fractionation efficiency. (**b**, upper panel) ErbB-2 (green) and Stat3 (red) were localized by IF and confocal microscopy. Merged images show HRGβ1-induced ErbB-2/Stat3 nuclear colocalization in yellow. Boxed areas are shown in detail in the inset. Nuclei were stained with 4′,6-diamidino-2-phenylindole (DAPI) (blue). Lower panel: Quantitative analysis of NErbB-2 levels in confocal images from upper panel. Fluorescence intensities of NErbB-2 were quantified and are expressed as the percentage of NErbB-2 (mean ± s.d., $n = 50$ from each group). (**c**) Nuclear extracts were immunoprecipitated (IP) with ErbB-2, Stat3 or IgG (as control of specificity) antibodies, and analyzed by WB with the indicated p-antibodies. Membranes were reprobed with total antibodies. Total cell lysates were blotted in parallel. (**d** and **e**) ErbB-2 (red) and ErbB-3 or HRG (green) were localized by IF; data are shown as detailed in (**b**). Merged images show HRGβ1-induced ErbB-2/ErbB-3 (**d**) or ErbB-2/HRG (**e**) nuclear colocalization in yellow. Lower panel in (**d**) shows quantitative analysis of NErbB-3 levels in confocal images. (**f**) Nuclear extracts were IP with ErbB-2, ErbB-3 or IgG antibodies, and analyzed by WB with the indicated antibodies. Total lysates were blotted in parallel. (**g** and **h**) ErbB-2, Stat3 and ErbB-3 were localized by IF in BT-474 and JIMT-1 cells; data are shown as in (**b** and **d**), respectively. (**i**) Effect of hErbB-2ΔNLS on ErbB-3 nuclear migration. hErbB-2ΔNLS-transfected cells were treated with HRGβ1. GFP from hErbB-2ΔNLS was visualized by direct fluorescence imaging (green) and ErbB-3 (red) by IF. Solid arrows: hErbB-2ΔNLS-transfected cells; dashed arrows: wild-type cells that did not uptake the hErbB-2ΔNLS mutant. Experiments in (**a–i**) were repeated at least three times, with similar results (see Supplementary Figure S3).

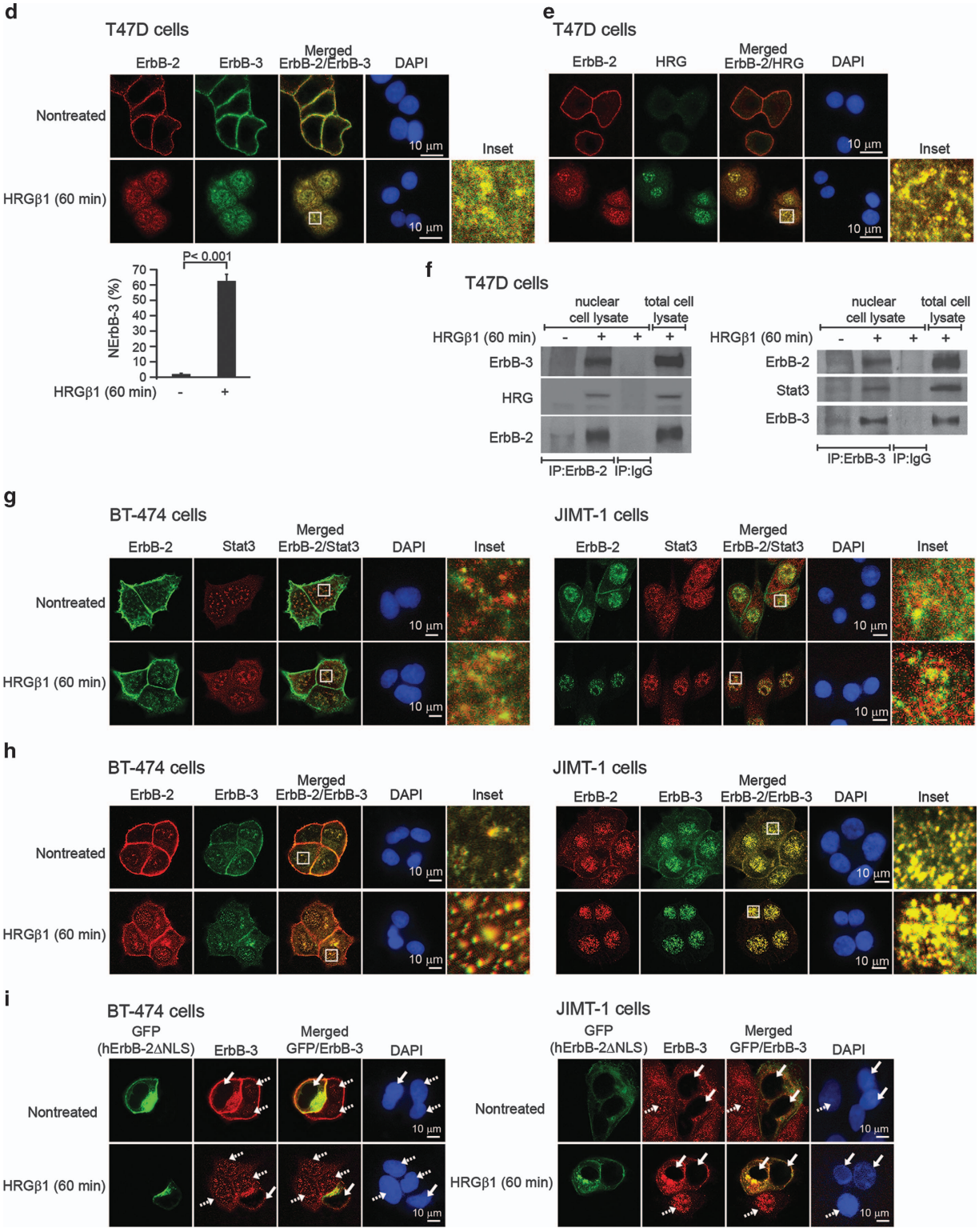

Figure 4. Continued.

the promoter (Figure 6a), consistent with hErbB-2ΔNLS ability to block ErbB-3 nuclear migration. Our study of the local chromatin architecture revealed that CBP, a coactivator with histone acetyltransferase activity, was recruited to the GAS site under basal conditions, and that HRGβ1 further stimulated its recruitment. Accordingly, basal levels of histone H3 acetylation were found, which were enhanced by HRGβ1 treatment (Figure 6a). Ttzm did not affect CBP recruitment or histone H3 acetylation levels. On the contrary, neither recruitment of CBP nor modification of histone H3 acetylation levels were observed in cells transfected with hErbB-2ΔNLS (Figure 6a). While Ttzm was unable to abolish HRGβ1-induced cyclin D1 protein and mRNA expression, transfer of hErbB-2ΔNLS blocked the said HRGβ1 effects (Figures 6b and c). These findings demonstrate that hErbB-2ΔNLS

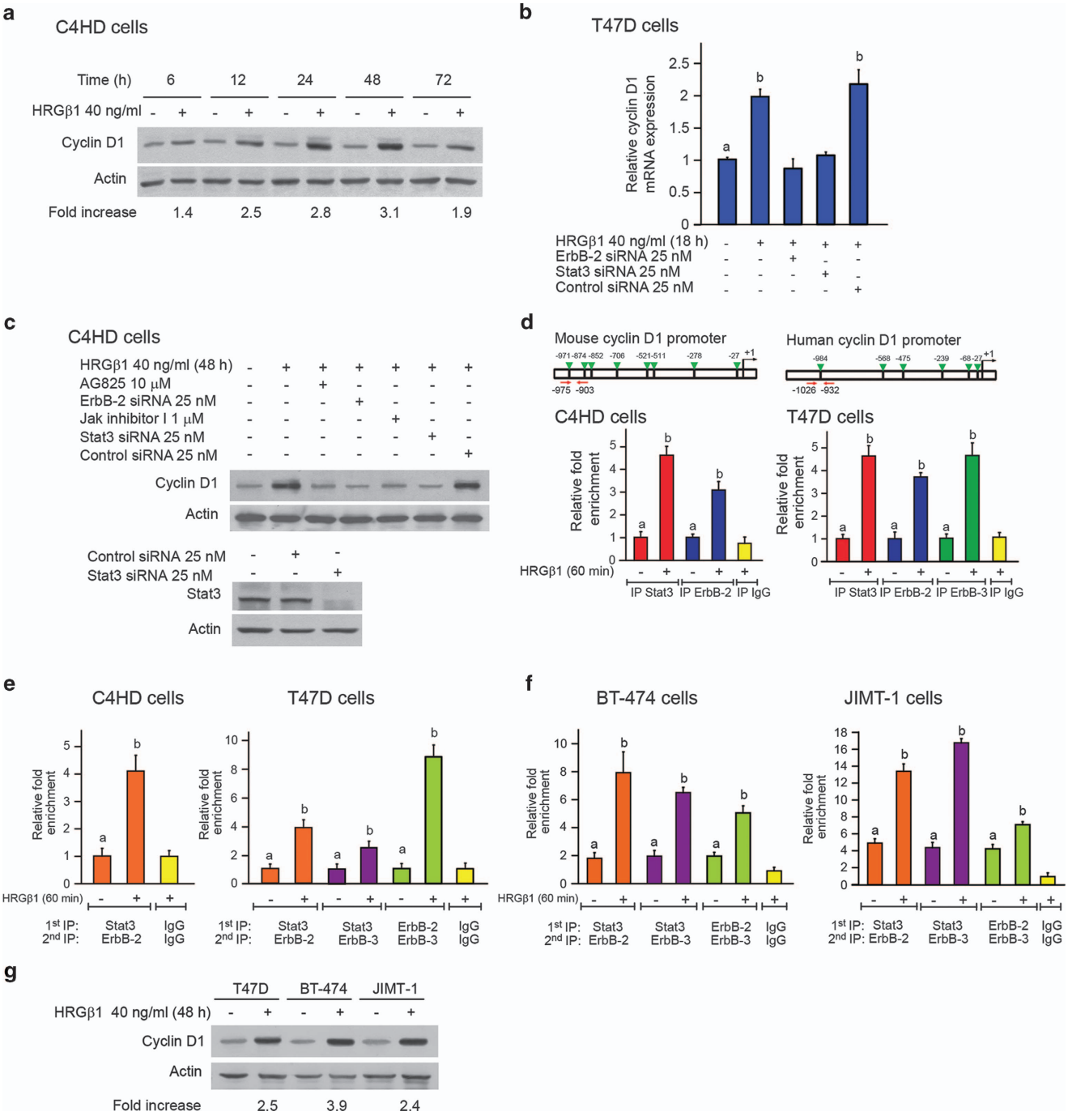

Figure 5. HRGβ1 induces the assembly of a Stat3/ErbB-2/ErbB-3 transcriptional complex at the cyclin D1 promoter in both Ttzm-sensitive and -resistant BC cells. (**a**) Cyclin D1 expression was analyzed by WB. (**b**) Cells were transfected with ErbB-2, Stat3 and control siRNAs and were treated with HRGβ1. Cyclin D1 mRNA expression levels were determined by RT–qPCR. Fold change of mRNA levels upon HRGβ1 treatment was calculated by normalizing the absolute levels of cyclin D1 mRNA to GAPDH levels, used as an internal control, setting the value of untreated cells as 1. Data are presented as mean ± s.e.m. For b vs a: $P < 0.001$. (**c**, upper panel) Cells were preincubated with the indicated pharmacologic inhibitors or transfected as in (**b**) and were treated with HRGβ1. Cyclin D1 levels were studied by WB. Lower panel: control of inhibition of Stat3 expression by siRNAs. Experiments in (**a**) to (**c**) were repeated three times, with similar results. (**d**) HRGβ1 induces *in vivo* binding of Stat3, ErbB-2 and ErbB-3 to the cyclin D1 promoter. Protein recruitment to cyclin D1 promoter was analyzed by ChIP in cells treated with HRGβ1. Immunoprecipitated DNA was amplified by qPCR using primers (red arrows) flanking the GAS sites (upper diagrams). Amounts of immunoprecipitated DNA were normalized to inputs and are reported relative to the amount obtained by IgG immunoprecipitation, used as a negative control, which was set to 1. Data are expressed as *n*-fold chromatin enrichment over IgG immunoprecipitation. For b vs a: $P < 0.001$. (**e**) Sequential ChIP. Chromatins were first immunoprecipitated with Stat3 or ErbB-2 antibodies and were reimmunoprecipitated using ErbB-2 or ErbB-3 antibodies. qPCR and data analysis were performed as in (**d**). For b vs a: $P < 0.001$. (**f**) Sequential ChIP assays were performed in BT-474 and JIMT-1 cells as in (**e**). Immunoprecipitated DNA was amplified by qPCR using primers flanking the GAS site at − 984 shown in (**d**). Results in (**d**–**f**) are mean ± s.e.m. from three independent experiments. (**g**) Cyclin D1 expression was analyzed by WB. As control, T47D cells were blotted in parallel. The experiment shown was repeated three times with similar results (see Supplementary Figure S4).

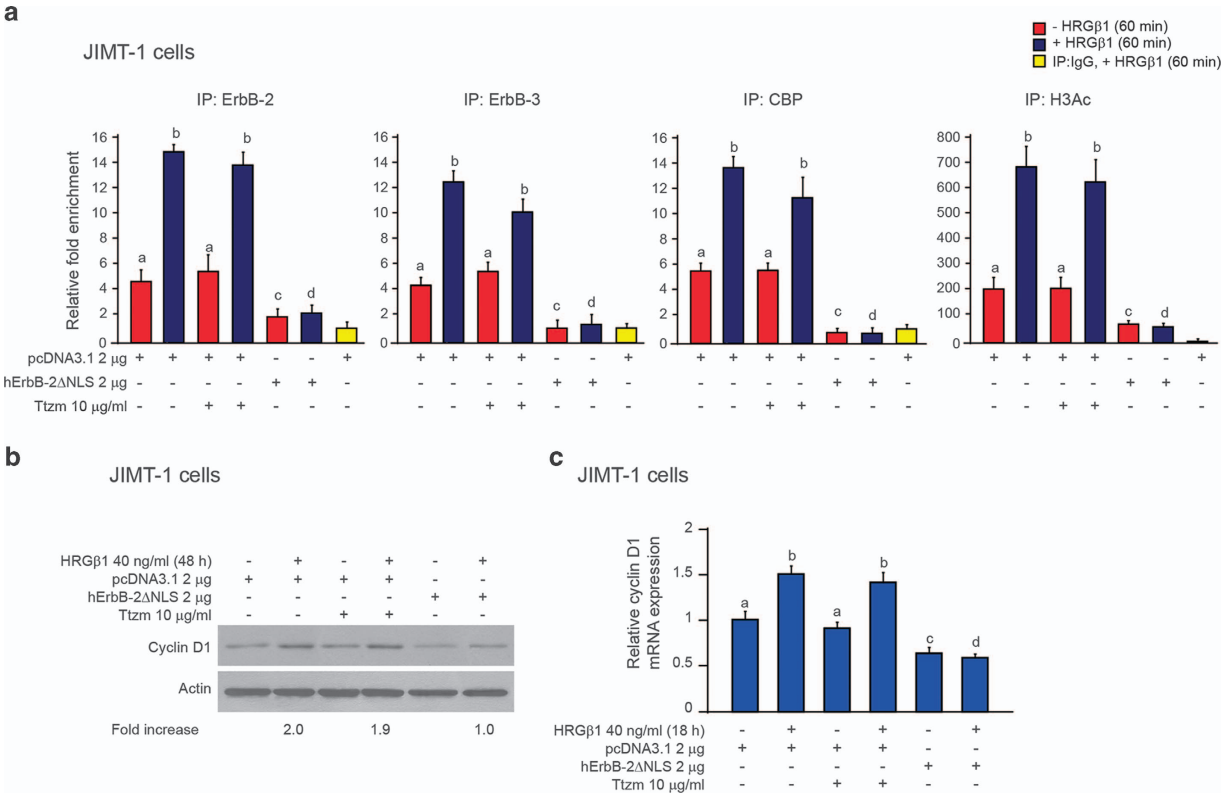

Figure 6. Disruption of the Stat3/ErbB-2/ErbB-3 nuclear complex is the differential molecular signature underlying hErbB-2ΔNLS growth inhibitory effects in Ttzm-resistant cells. (**a**) The hErbB-2ΔNLS abolishes the assembly of the ErbB-2/ErbB-3 complex at the cyclin D1 promoter. Cells were transfected with the hErbB-2ΔNLS or pcDNA3.1 vector. When indicated, cells were pretreated with Ttzm and were then treated with HRGβ1 or remained untreated. Recruitment of ErbB-2, ErbB-3 and CBP, and H3 acetylation levels (H3Ac) at the cyclin D1 promoter was analyzed by ChIP. IgG immunoprecipitation was used as a negative control. Immunoprecipitated DNA was amplified by qPCR using primers flanking the GAS site at position − 984, shown in Figure 5. Amounts of immunoprecipitated DNA were normalized to inputs and are reported relative to the amount obtained by IgG immunoprecipitation, which was set to 1. For b and c vs a, and d vs b: $P < 0.001$. Data represent the means of data from three independent experiments ± s.e.m. (**b**) Cyclin D1 protein levels in cells treated as described in (**a**) were analyzed by WB as in Figure 5. (**c**) Cyclin D1 mRNA expression levels in cells treated as in (**a**) were determined by RT–qPCR. Data analysis was performed as in Figure 5. Data are presented as mean ± s.e.m. For b and c vs a, and d vs b: $P < 0.001$. Experiments in (**b**) and (**c**) were repeated three times, with similar results.

inhibitory effects on Ttzm-resistant JIMT-1 cells lies in the disruption of the Stat3/ErbB-2/ErbB-3 nuclear complex driving cyclin D1 expression.

ErbB-2 and Stat3 nuclear coexpression is associated with poor clinical outcome

We explored the clinical significance of ErbB-2 and Stat3 nuclear coexpression in tissue microarrays from 42 MErbB-2-overexpressing primary breast tumors. The clinical and pathological characteristics of these specimens are shown in Supplementary Table S1. In this cohort, 22 patients belong to the luminal B-like, HER2-positive (estrogen receptor (ER)- and/or progesterone receptor (PR)-positive, MErbB-2-overexpressed) BC subtype and 19 to the HER2-positive, non-luminal (ER- and PR-negative, MErbB-2-overexpressed) subtype, according to the surrogate definitions of intrinsic BC subtypes[48] (Supplementary Table S1). Here, MErbB-2 was studied by immunohistochemistry and immunofluorescence (IF)[49,50] and NErbB-2 by IF, and scored as we reported.[49] NStat3 was studied by IF[20] and scored as NErbB-2,[49] considering the percentage of positive cells and staining intensity (Supplementary Figure S5 details scoring). Scores of 2+ and 3+ were considered positive for NErbB-2,[49] and of 1+ to 3+, positive for NStat3[51] (Supplementary Figure S5). Among 11 tumors expressing NErbB-2, nine also coexpressed NStat3 (81%, 95% confidence interval = 48–97). Representative samples are shown in Figure 7a. NErbB-2/NStat3 coexpression was significantly associated with higher clinical stage in our total cohort of MErbB-2-overexpressing tumors (Supplementary Table S2). No significant correlation between the BC subtype and NErbB-2/NStat3 coexpression was found (Supplementary Table S2). Kaplan–Meier analysis revealed that coexpression correlated with lower overall survival (Figure 7b). These results validate in the clinic our findings on the key role of the NErbB-2/NStat3 complex as driver of proliferation in ErbB-2-positive BC.

DISCUSSION

Our findings challenge the paradigm of anti-ErbB-2 drug design, revealing that blockade of NErbB-2 presence abrogates growth of BC sensitive and resistant to Ttzm. We found that ErbB-2 assembly of a transcriptional complex with ErbB-3 and Stat3 at the cyclin D1 promoter modulates basal and HRGβ1-induced BC growth. Our results highlight nuclear ErbB-2 as the major driver of proliferation in Ttzm-resistant BC and demonstrate that Ttzm inability to disrupt the Stat3/ErbB-2/ErbB-3 transcriptional complex and cyclin D1 expression underlies its failure to inhibit BC growth.

Increasingly, strong evidence, including ours, revealed nuclear presence and function of ErbB-2, as well as of other ErbB family members and their ligands in BC.[6,19–24] We also identified NErbB-2 positivity as an independent prognostic factor of worse overall survival in patients with MErbB-2 overexpression.[49] In spite of these

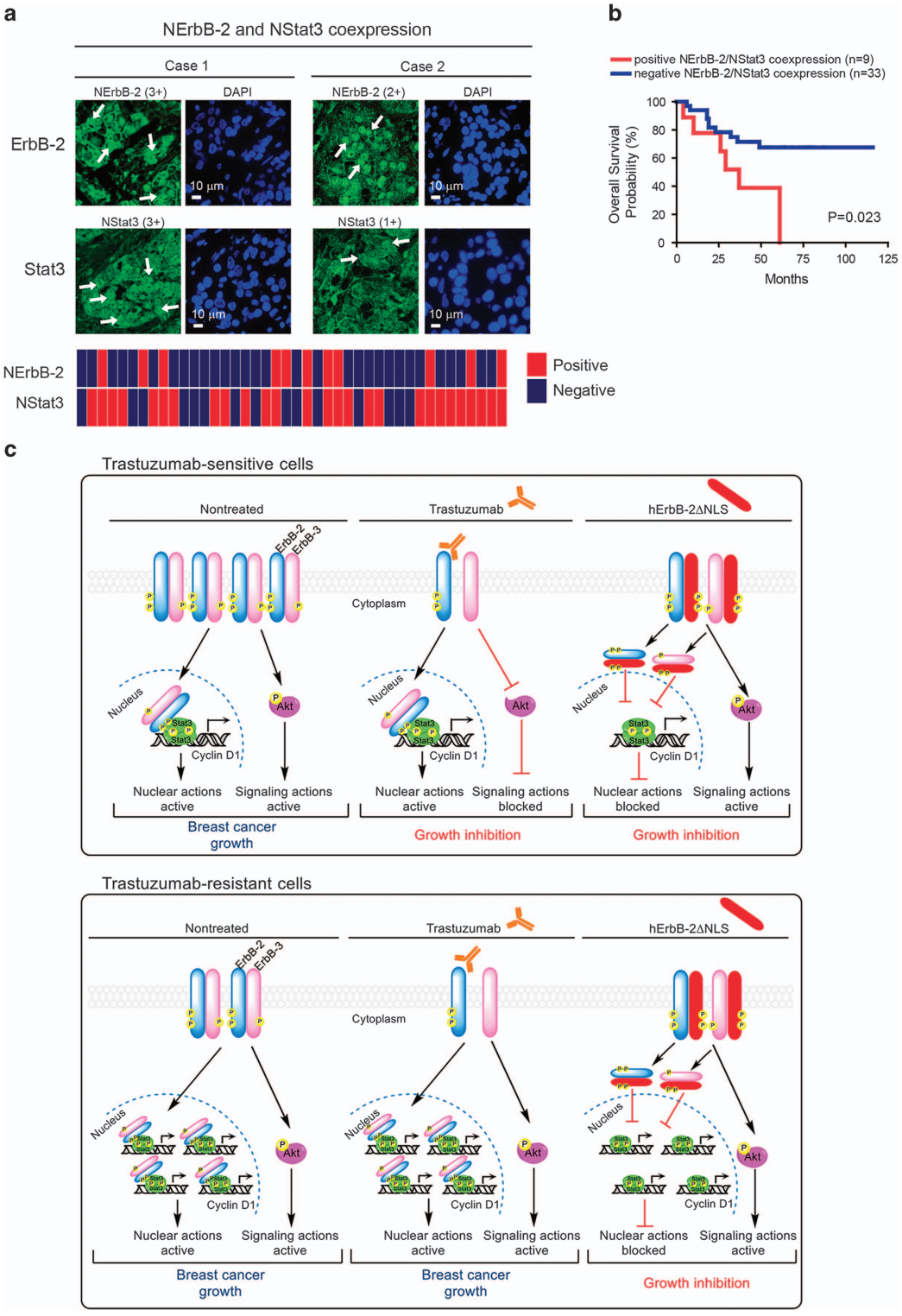

Figure 7. ErbB-2 and Stat3 nuclear coexpression is associated with poor clinical outcome. (**a**) NErbB-2 and NStat3 coexpression in tumor samples. Upper panel: NErbB-2 and NStat3 levels were evaluated by IF and scored as described in Results. Shown are examples of tumors showing positive NErbB-2/NStat3 coexpression. Nuclei were stained with 4′,6-diamidino-2-phenylindole (DAPI). Lower panel: A schematic overview of the tissue microarrays (TMAs) and a summary of the IF results are shown. Positive specimens are shown in red and negative specimens, in blue. (**b**) Kaplan–Meier survival analysis and log-rank test were performed to correlate NErbB-2/NStat3 coexpression with overall patient survival in MErbB-2-overexpressing patients. (**c**) Model of Ttzm and hErbB-2ΔNLS action. Ttzm-sensitive cells display higher levels of MErbB-2 than of NErbB-2 and their proliferation is driven by signaling (e.g. PI3K/AKT) and nuclear (e.g. Stat3/ErbB-2/ErbB-3 transcriptional complex at cyclin D1 promoter) ErbB-2 actions, both hierarchically equal. Inhibition of signaling with Ttzm or of nuclear action with hErbB-2ΔNLS blocks proliferation. Ttzm-resistant cells display high levels of NErbB-2, which indeed may be higher than those of MErbB-2. NErbB-2 role on proliferation is stronger than that of MErbB-2. Therefore, inhibition of NErbB-2 effect with hErbB-2ΔNLS blocks BC growth even in the presence of signaling pathways' activation (see Supplementary Figure S5 and Supplementary Tables S1 and S2).

experimental and clinical findings, the current anti-ErbB-2 therapy with Ttzm targets only MErbB-2. *De novo* or acquired resistance to Ttzm is still a major clinical issue.[52,53] Where Ttzm failed, other therapies have proved efficient, like pertuzumab, which inhibits ligand-induced ErbB-2/ErbB-3 heterodimerization,[29,54] and the kinase inhibitor lapatinib.[55,56] Yet again, both target only MErbB-2.

Our BC models display multiple mechanisms of Ttzm failure. HRG induces the assembly of ErbB-2/ErbB-3 dimers insensitive to Ttzm disruption in BT-474 and SK-BR-3 cells.[29,34] Owing to either activating mutations in *PIK3CA* or decreased levels of the PTEN phosphatase, PI3K/AKT activation is a mechanism of resistance[26,27] present in all Ttzm-unresponsive lines we studied.[41,57] HCC1419 cells express a constitutively active truncated ErbB-2, which correlates with lack of Ttzm effect.[41,58] Increased EGF-R expression and phosphorylation and high levels of ErbB ligands have been identified as a mechanism of acquired Ttzm resistance in BT-474 cells.[42] We here revealed increased NErbB-2 expression as a novel common feature underlying intrinsic and acquired Ttzm resistance. Most of the intrinsic Ttzm-resistant cells we studied showed higher levels of NErbB-2 than of MErbB-2. Also, HRGβ1-conferred resistance correlates with an inversion of MErbB-2/NErbB-2 ratios or with a striking increase in NErbB-2 levels. Similarly, acquired resistance in BT-474 cells resulted in higher NErbB-2 content than that in their sensitive counterparts. As regards the response to anti-ErbB-2 therapies, our results suggest that the concept of ErbB-2 overexpression should be extended to include NErbB-2 levels.

In all Ttzm-responsive and -resistant human BC lines studied, we found basal nuclear ErbB-2, ErbB-3 and Stat3, as well as ErbB-2/ErbB-3 and ErbB-2/Stat3 nuclear colocalization, which was increased by HRGβ1. Basal MErbB-2/MErbB-3 dimers were more numerous in sensitive cells than in resistant cells, and conversely, nuclear dimers were more abundant in resistant cells, suggesting a role of nuclear ErbB dimers in Ttzm response. Indeed, our mechanistic studies revealed basal and HRGβ1-induced assembly of a Stat3/ErbB-2/ErbB-3 transcriptional complex at the GAS sites of the cyclin D1 promoter, where ErbB-2 and ErbB-3 act as Stat3 cofactors. Although MErbB-2 and HRG involvement in cyclin D1 expression via signaling pathways has been found,[59–62] this is the first report of a nuclear function of the ErbB-2/ErbB-3 dimer, resulting in the regulation of cyclin D1 expression. Nuclear ErbB-3 was detected in mammary epithelial and BC cells.[6,23,24,63] Recently, the full-length and a 80 kDa ErbB-3 variant were found recruited to cyclin D1 promoter regions with multiple GAS sites, including the one studied here,[20,64] and to induce said regions' transcriptional activity in BC cells.[24,65] ErbB-3-response elements have not yet been characterized, which prevents the determination of whether ErbB-3 is bound directly to DNA. Our findings raise the possibility that in these reports ErbB-3 was loaded as cofactor of Stat3 at said promoter regions enriched in GAS sites. The presence of several HRG isoforms in the nucleus of BC cells and primary tumors has already been reported.[21,22] However, the biologic function of nuclear HRG in BC remains poorly known. While nuclear HRGβ1 appears to be involved in the induction of gene expression, HRGα functions as a transrepressor in luciferase reporter assays.[21,66] Our findings revealed that at the nuclear compartment, HRGβ1 remains bound to ErbB-3, its cognate receptor, and assembles a transcriptional complex with ErbB-2 and Stat3, which modulates cyclin D1 expression and BC growth.

In line with NErbB-2 central role in BC growth, we found that inhibition of ErbB-2 nuclear localization by transfer of hErbB-2ΔNLS blocks *in vitro* and *in vivo* HRGβ1-induced growth of a MErbB-2-overexpressing BC mouse model, basal and HRGβ1-stimulated *in vitro* growth of ErbB-2-amplified human BC cells, both Ttzm-sensitive and -resistant, and proliferation of a preclinical model of Ttzm-resistant BC. Our comparative studies on hErbB-2ΔNLS and Ttzm effects showed that inhibition of ErbB-2 nuclear localization abolishes basal and HRGβ1-stimulated growth of ErbB-2-positive BC in the presence of ErbB-2/ErbB-3 dimers, ErbB-3 phosphorylation and PI3K/AKT pathway activation, conditions where Ttzm is inefficient.[27,29,34,38] On the other hand, Ttzm was unable to block basal and HRGβ1-stimulated NErbB-2 presence. Disruption of the Stat3/ErbB-2/ErbB-3 complex governing cyclin D1 expression was the differential molecular signature underlying growth inhibitory effects of hErbB-2ΔNLS in Ttzm-resistant BC. Our results are consistent with a model (Figure 7c) where, in cells displaying higher levels of MErbB-2 than of NErbB-2, proliferation is driven by signaling and nuclear ErbB actions, both hierarchically equal. Inhibition of signaling with Ttzm or of nuclear actions with hErbB-2ΔNLS would block proliferation. Contrastingly, in BC cells displaying high levels of NErbB-2, which may be basally higher than those of MErbB-2 or may be increased by HRGβ1 treatment, NErbB-2 role on proliferation is stronger than that of MErbB-2. Thus, inhibition of NErbB-2 action would be the appropriate strategy to block proliferation (Figure 7c).

Our clinical findings showed that NErbB-2/NStat3 interaction correlates with poor clinical outcome in MErbB-2-overexpressing BC. Interestingly, the said interaction is not restricted to the HER2-positive (non-luminal) BC subtype, but occurs also in luminal B-like HER2-positive tumors. This finding indicates that NErbB-2/NStat3 coexpression may serve as a new biomarker of prognosis in all breast tumors overexpressing MErbB-2. Our present results in experimental models and in the clinic reveal the blockade of NErbB-2 localization as a novel strategy in BC cells expressing high NErbB-2 levels.

MATERIALS AND METHODS

Animals and tumors

BALB/c mice studies were conducted as outlined in the NIH Guide for the Care and Use of Laboratory Animals and were approved by the IBYME Animal Research Committee.[20]

Antibodies and reagents

Antibodies and reagents are listed under Supplementary Materials and methods.

Cell lines, treatments and proliferation assays

C4HD epithelial cells from the model of mammary carcinogenesis induced by medroxyprogesterone acetate in mice overexpress ErbB-2 and ErbB-3, exhibit low ErbB-4 levels and lack EGF-R expression.[9] These cells also display high levels of ER and PR.[9] BT-474, SK-BR-3 and T47D cells were obtained from American Type Culture Collection (Manassas, VA, USA), and JIMT-1 cells were from the German Tissue Repository DSMZ (Braunschweig, Germany). MDA-MB-453, HCC1569 and HCC1419 were a gift from DJ Slamon (University of California, Los Angeles, CA, USA). BT-474HR clone, selected for its resistance to Ttzm, was obtained following the previously described protocol.[42] Primary cultures of epithelial cells from C4HD tumors were performed as described.[9] BT-474, SK-BR-3, BT-474HR and T47D cells were cultured as described previously.[11,20,67,68] JIMT-1 cells were maintained in DMEM-F12 (Dulbecco's modified Eagle's medium/nutrient mixture F12) supplemented with 10% fetal calf serum. MDA-MB-453, HCC1569 and HCC1419 cells were cultured as described by DJ Slamon.[41] All cell types were starved in 0.1% charcoalized fetal calf serum for 48 h before stimulation with HRGβ1 (40 ng/ml), or were pretreated with Ttzm (10 μg/ml), AG825 (10 or 100 μM) or Jak inhibitor I (1 μM) for 90 min before HRGβ1 stimulation. In experiments assessing the effects of mutant ErbB-2 (hErbB-2ΔNLS), cells were transfected as described with the corresponding plasmid or pcDNA3.1 empty plasmid for 24 h before HRGβ1 treatment.[20] Proliferation was evaluated by [^{3}H]thymidine incorporation assay or cell count, and cell cycle distribution was evaluated by flow cytometry.[20,69]

Western blot analysis and immunoprecipitation assays

Sodium dodecyl sulfate–polyacrylamide gel electrophoresis and immunoblots were performed as described.[20] The association among ErbB-2, ErbB-3 and Stat3 was studied by co-immunoprecipitation experiments using 500 μg of nuclear or total cell lysates as described.[20] A detailed

description of western blot (WB) analysis is provided in Supplementary Materials and methods.

Plasmids and transient transfections

Plasmids and siRNA sequences are detailed under Supplementary Materials and methods. Fugene HD transfection technique (Roche Biochemicals, Indianapolis, IN, USA) was performed as described.[20] Transfection of siRNA duplexes was performed for 3 days by using DharmaFECT transfection reagent (Dharmacon, Lafayette, CO, USA) according to the manufacturer's instructions. For reconstitution experiments, co-transfection of 25 nM ErbB-2 siRNA with 2 μg expression vectors was performed using DharmaFECT Duo transfection reagent (Dharmacon).

IF and confocal microscopy in cell cultures

Techniques were performed as we already described.[20] Cells were analyzed using a Nikon Eclipse E800 confocal laser microscopy system.[20] A detailed description of antibodies used and of quantitative analysis of confocal images is provided in Supplementary Materials and methods.

ChIP and sequential ChIP assays

ChIP and sequential ChIP assays were performed as we described.[20] Primers used are listed in Supplementary Materials and methods.

RNA preparation and real-time quantitative RT–PCR

RNA was obtained and cyclin D1 mRNA levels were detected as we described.[20] Primers used are listed in Supplementary Materials and methods.

Preclinical models

C4HD cells were transfected with pcDNA3.1 or hErbB-2ΔNLS vectors and 10^6 cells from each group ($n = 6$) were inoculated subcutaneously into NIH (S) nude mice (La Plata University, La Plata, Buenos Aires, Argentina) treated with a 5 μg HRGβ1 slow-release pellet as described under Supplementary Materials and methods. Tumor volume, growth rate and growth delay were determined as described.[20] Comparison of tumor volumes between different groups was carried out by analysis of variance followed by Tukey's test. Linear regression analysis was performed on tumor growth curves, and the slopes were compared using analysis of variance followed by a parallelism test to evaluate the statistical significance of differences.

JIMT-1 cells were transfected with expression vectors and 4×10^6 cells from each group were inoculated subcutaneously into NIH(S) nude mice. When tumors developed from pcDNA3.1-transfected cells reached 40 mm^3, animals were divided into three groups ($n = 8$) and injected with Ttzm (20 mg/kg, intraperitoneally), or with human IgG as control (20 mg/kg, intraperitoneally) two times a week, or remained untreated. Tumor volume, growth rate and growth delay were determined as explained.

Patients and tissue microarrays

We selected 42 MErbB-2-overexpressing paraffin-embedded tissue samples from a cohort of archived invasive breast carcinomas from the files of the Histopathology Department of Temuco Hospital, Chile, from 1998 to 2006.[49] This study was conducted with the approval of the Institutional Review Board on Human Research of Universidad de La Frontera. Details of informed consents, pretreatment staging of patients, treatments, tissue microarray construction and IF analysis are provided in Supplementary Materials and methods.

Statistics

Analyses were performed using STATA version 11 software (Stata Corp., College Station, TX, USA). Correlations between categorical variables were performed using Fisher's exact test. Cumulative overall survival probabilities were calculated according to the Kaplan–Meier method, and statistical significance was analyzed by log-rank test. All the tests of statistical significance were two-sided. *P*-values < 0.05 were regarded as statistically significant.

CONFLICT OF INTEREST

The authors declare no conflict of interest.

ACKNOWLEDGEMENTS

We thank Mien-Chie Hung (MD Anderson Cancer Center, Houston, TX, USA) for his generous gift of the hErbB-2ΔNLS, which indeed made this work possible, and AA Molinolo (NIH, Bethesda, MD, USA) for his constant help and support. We also thank J Giudice (Baylor College of Medicine, Houston, TX, USA) for help with quantification of confocal images, and V Chiauzzi for her excellent technical assistance. This work was supported by the Susan G Komen for the Cure KG090250 investigator-initiated research Grant, IDB/PICT 2012-668 and PID 2012-066 from the National Agency of Scientific Promotion of Argentina (all of them awarded to PVE), IDB/PICT 2012-382 from the National Agency of Scientific Promotion of Argentina (awarded to RS) and Oncomed-Reno CONICET 1819/03, from the Henry Moore Institute of Argentina (awarded to PVE and RS).

AUTHOR CONTRIBUTIONS

PVE, RICR and WB were responsible for the conception and design of the study. RICR and WB contributed equally to this work. PVE, WB, RICR, MCDF, CJP, PG and RS developed methodology. RICR, WB, PVE, MCDF, CJP, LV, NG, MT, PG, NAO, JCR, RS and EHC acquired the data (and also provided animals, acquired and managed patients, provided facilities, etc.). PVE, RICR, WB, RS, PG and JCR analyzed and interpreted the data. PVE wrote the manuscript with assistance from RICR. PVE supervised the study. All authors read and approved the final manuscript.

REFERENCES

1 Slamon DJ, Godolphin W, Jones LA, Holt JA, Wong SG, Keith DE *et al.* Studies of the HER-2/neu proto-oncogene in human breast and ovarian cancer. *Science* 1989; **244**: 707–712.
2 Henderson IC, Patek AJ. The relationship between prognostic and predictive factors in the management of breast cancer. *Breast Cancer Res Treat* 1998; **52**: 261–288.
3 Ross JS, Slodkowska EA, Symmans WF, Pusztai L, Ravdin PM, Hortobagyi GN. The HER-2 receptor and breast cancer: ten years of targeted anti-HER-2 therapy and personalized medicine. *Oncologist* 2009; **14**: 320–368.
4 Tzahar E, Waterman H, Chen X, Levkowitz G, Karunagaran D, Lavi S *et al.* A hierarchical network of interreceptor interactions determines signal transduction by Neu differentiation factor/neuregulin and epidermal growth factor. *Mol Cell Biol* 1996; **16**: 5276–5287.
5 Landgraf R. HER2 therapy. HER2 (ERBB2): functional diversity from structurally conserved building blocks. *Breast Cancer Res* 2007; **9**: 202.
6 Tao RH, Maruyama IN. All EGF (ErbB) receptors have preformed homo- and heterodimeric structures in living cells. *J Cell Sci* 2008; **121**: 3207–3217.
7 Lee-Hoeflich ST, Crocker L, Yao E, Pham T, Munroe X, Hoeflich KP *et al.* A central role for HER3 in HER2-amplified breast cancer: implications for targeted therapy. *Cancer Res* 2008; **68**: 5878–5887.
8 Holbro T, Beerli RR, Maurer F, Koziczak M, Barbas CF III, Hynes NE. The ErbB2/ErbB3 heterodimer functions as an oncogenic unit: ErbB2 requires ErbB3 to drive breast tumor cell proliferation. *Proc Natl Acad Sci USA* 2003; **100**: 8933–8938.
9 Balana ME, Lupu R, Labriola L, Charreau EH, Elizalde PV. Interactions between progestins and heregulin (HRG) signaling pathways: HRG acts as mediator of progestins proliferative effects in mouse mammary adenocarcinomas. *Oncogene* 1999; **18**: 6370–6379.
10 Salatino M, Schillaci R, Proietti CJ, Carnevale R, Frahm I, Molinolo AA *et al.* Inhibition of *in vivo* breast cancer growth by antisense oligodeoxynucleotides to type I insulin-like growth factor receptor mRNA involves inactivation of ErbBs, PI-3K/Akt and p42/p44 MAPK signaling pathways but not modulation of progesterone receptor activity. *Oncogene* 2004; **23**: 5161–5174.
11 Proietti CJ, Rosemblit C, Beguelin W, Rivas MA, Diaz Flaque MC, Charreau EH *et al.* Activation of Stat3 by heregulin/ErbB-2 through the co-option of progesterone receptor signaling drives breast cancer growth. *Mol Cell Biol* 2009; **29**: 1249–1265.
12 Labriola L, Salatino M, Proietti CJ, Pecci A, Coso OA, Kornblihtt AR *et al.* Heregulin induces transcriptional activation of the progesterone receptor by a mechanism that requires functional ErbB-2 and mitogen-activated protein kinase activation in breast cancer cells. *Mol Cell Biol* 2003; **23**: 1095–1111.

13 Alimandi M, Romano A, Curia MC, Muraro R, Fedi P, Aaronson SA *et al.* Cooperative signaling of ErbB3 and ErbB2 in neoplastic transformation and human mammary carcinomas. *Oncogene* 1995; **10**: 1813–1821.
14 Chiu CG, Masoudi H, Leung S, Voduc DK, Gilks B, Huntsman DG *et al.* HER-3 overexpression is prognostic of reduced breast cancer survival: a study of 4046 patients. *Ann Surg* 2010; **251**: 1107–1116.
15 Hsieh AC, Moasser MM. Targeting HER proteins in cancer therapy and the role of the non-target HER3. *Br J Cancer* 2007; **97**: 453–457.
16 Slamon DJ, Leyland-Jones B, Shak S, Fuchs H, Paton V, Bajamonde A *et al.* Use of chemotherapy plus a monoclonal antibody against HER2 for metastatic breast cancer that overexpresses HER2. *N Engl J Med* 2001; **344**: 783–792.
17 Smith I, Procter M, Gelber RD, Guillaume S, Feyereislova A, Dowsett M *et al.* 2-year follow-up of trastuzumab after adjuvant chemotherapy in HER2-positive breast cancer: a randomised controlled trial. *Lancet* 2007; **369**: 29–36.
18 Esteva FJ, Valero V, Booser D, Guerra LT, Murray JL, Pusztai L *et al.* Phase II study of weekly docetaxel and trastuzumab for patients with HER-2-overexpressing metastatic breast cancer. *J Clin Oncol* 2002; **20**: 1800–1808.
19 Wang SC, Lien HC, Xia W, Chen IF, Lo HW, Wang Z *et al.* Binding at and transactivation of the COX-2 promoter by nuclear tyrosine kinase receptor ErbB-2. *Cancer Cell* 2004; **6**: 251–261.
20 Beguelin W, Diaz Flaque MC, Proietti CJ, Cayrol F, Rivas MA, Tkach M *et al.* Progesterone receptor induces ErbB-2 nuclear translocation to promote breast cancer growth via a novel transcriptional effect: ErbB-2 function as a coactivator of Stat3. *Mol Cell Biol* 2010; **30**: 5456–5472.
21 Li W, Park JW, Nuijens A, Sliwkowski MX, Keller GA. Heregulin is rapidly translocated to the nucleus and its transport is correlated with c-myc induction in breast cancer cells. *Oncogene* 1996; **12**: 2473–2477.
22 Marshall C, Blackburn E, Clark M, Humphreys S, Gullick WJ. Neuregulins 1-4 are expressed in the cytoplasm or nuclei of ductal carcinoma (*in situ*) of the human breast. *Breast Cancer Res Treat* 2006; **96**: 163–168.
23 Offterdinger M, Schofer C, Weipoltshammer K, Grunt TW. C-erbB-3: a nuclear protein in mammary epithelial cells. *J Cell Biol* 2002; **157**: 929–939.
24 Brand TM, Iida M, Luthar N, Wleklinski MJ, Starr MM, Wheeler DL. Mapping C-terminal transactivation domains of the nuclear HER family receptor tyrosine kinase HER3. *PLoS ONE* 2013; **8**: e71518.
25 Giri DK, Ali-Seyed M, Li LY, Lee DF, Ling P, Bartholomeusz G *et al.* Endosomal transport of ErbB-2: mechanism for nuclear entry of the cell surface receptor. *Mol Cell Biol* 2005; **25**: 11005–11018.
26 Berns K, Horlings HM, Hennessy BT, Madiredjo M, Hijmans EM, Beelen K *et al.* A functional genetic approach identifies the PI3K pathway as a major determinant of trastuzumab resistance in breast cancer. *Cancer Cell* 2007; **12**: 395–402.
27 Nagata Y, Lan KH, Zhou X, Tan M, Esteva FJ, Sahin AA *et al.* PTEN activation contributes to tumor inhibition by trastuzumab, and loss of PTEN predicts trastuzumab resistance in patients. *Cancer Cell* 2004; **6**: 117–127.
28 Agus DB, Akita RW, Fox WD, Lewis GD, Higgins B, Pisacane PI *et al.* Targeting ligand-activated ErbB2 signaling inhibits breast and prostate tumor growth. *Cancer Cell* 2002; **2**: 127–137.
29 Junttila TT, Akita RW, Parsons K, Fields C, Lewis Phillips GD, Friedman LS *et al.* Ligand-independent HER2/HER3/PI3K complex is disrupted by trastuzumab and is effectively inhibited by the PI3K inhibitor GDC-0941. *Cancer Cell* 2009; **15**: 429–440.
30 Wang YC, Morrison G, Gillihan R, Guo J, Ward RM, Fu X *et al.* Different mechanisms for resistance to trastuzumab versus lapatinib in HER2-positive breast cancers—role of estrogen receptor and HER2 reactivation. *Breast Cancer Res* 2011; **13**: R121.
31 Diermeier S, Horvath G, Knuechel-Clarke R, Hofstaedter F, Szollosi J, Brockhoff G. Epidermal growth factor receptor coexpression modulates susceptibility to Herceptin in HER2/neu overexpressing breast cancer cells via specific erbB-receptor interaction and activation. *Exp Cell Res* 2005; **304**: 604–619.
32 Li LY, Chen H, Hsieh YH, Wang YN, Chu HJ, Chen YH *et al.* Nuclear ErbB2 enhances translation and cell growth by activating transcription of ribosomal RNA genes. *Cancer Res* 2011; **71**: 4269–4279.
33 Yao E, Zhou W, Lee-Hoeflich ST, Truong T, Haverty PM, Eastham-Anderson J *et al.* Suppression of HER2/HER3-mediated growth of breast cancer cells with combinations of GDC-0941 PI3K inhibitor, trastuzumab, and pertuzumab. *Clin Cancer Res* 2009; **15**: 4147–4156.
34 Ghosh R, Narasanna A, Wang SE, Liu S, Chakrabarty A, Balko JM *et al.* Trastuzumab has preferential activity against breast cancers driven by HER2 homodimers. *Cancer Res* 2011; **71**: 1871–1882.
35 Lane HA, Beuvink I, Motoyama AB, Daly JM, Neve RM, Hynes NE. ErbB2 potentiates breast tumor proliferation through modulation of p27(Kip1)-Cdk2 complex formation: receptor overexpression does not determine growth dependency. *Mol Cell Biol* 2000; **20**: 3210–3223.
36 Graus-Porta D, Beerli RR, Daly JM, Hynes NE. ErbB-2, the preferred heterodimerization partner of all ErbB receptors, is a mediator of lateral signaling. *EMBO J* 1997; **16**: 1647–1655.
37 Daly JM, Olayioye MA, Wong AM, Neve R, Lane HA, Maurer FG *et al.* NDF/heregulin-induced cell cycle changes and apoptosis in breast tumour cells: role of PI3 kinase and p38 MAP kinase pathways. *Oncogene* 1999; **18**: 3440–3451.
38 Yakes FM, Chinratanalab W, Ritter CA, King W, Seelig S, Arteaga CL. Herceptin-induced inhibition of phosphatidylinositol-3 kinase and Akt Is required for antibody-mediated effects on p27, cyclin D1, and antitumor action. *Cancer Res* 2002; **62**: 4132–4141.
39 Tanner M, Kapanen AI, Junttila T, Raheem O, Grenman S, Elo J *et al.* Characterization of a novel cell line established from a patient with Herceptin-resistant breast cancer. *Mol Cancer Ther* 2004; **3**: 1585–1592.
40 Koninki K, Barok M, Tanner M, Staff S, Pitkanen J, Hemmila P *et al.* Multiple molecular mechanisms underlying trastuzumab and lapatinib resistance in JIMT-1 breast cancer cells. *Cancer Lett* 2010; **294**: 211–219.
41 O'Brien NA, Browne BC, Chow L, Wang Y, Ginther C, Arboleda J *et al.* Activated phosphoinositide 3-kinase/AKT signaling confers resistance to trastuzumab but not lapatinib. *Mol Cancer Ther* 2010; **9**: 1489–1502.
42 Ritter CA, Perez-Torres M, Rinehart C, Guix M, Dugger T, Engelman JA *et al.* Human breast cancer cells selected for resistance to trastuzumab *in vivo* overexpress epidermal growth factor receptor and ErbB ligands and remain dependent on the ErbB receptor network. *Clin Cancer Res* 2007; **13**: 4909–4919.
43 Barok M, Tanner M, Koninki K, Isola J. Trastuzumab-DM1 causes tumour growth inhibition by mitotic catastrophe in trastuzumab-resistant breast cancer cells *in vivo*. *Breast Cancer Res* 2011; **13**: R46.
44 Leow CC, Chesebrough J, Coffman KT, Fazenbaker CA, Gooya J, Weng D *et al.* Antitumor efficacy of IPI-504, a selective heat shock protein 90 inhibitor against human epidermal growth factor receptor 2-positive human xenograft models as a single agent and in combination with trastuzumab or lapatinib. *Mol Cancer Ther* 2009; **8**: 2131–2141.
45 Bromberg JF, Horvath CM, Besser D, Lathem WW, Darnell JE Jr. Stat3 activation is required for cellular transformation by v-src. *Mol Cell Biol* 1998; **18**: 2553–2558.
46 Bromberg JF, Wrzeszczynska MH, Devgan G, Zhao Y, Pestell RG, Albanese C *et al.* Stat3 as an oncogene. *Cell* 1999; **98**: 295–303.
47 Maegawa M, Takeuchi K, Funakoshi E, Kawasaki K, Nishio K, Shimizu N *et al.* Growth stimulation of non-small cell lung cancer cell lines by antibody against epidermal growth factor receptor promoting formation of ErbB2/ErbB3 heterodimers. *Mol Cancer Res* 2007; **5**: 393–401.
48 Goldhirsch A, Winer EP, Coates AS, Gelber RD, Piccart-Gebhart M, Thurlimann B *et al.* Personalizing the treatment of women with early breast cancer: highlights of the St Gallen International Expert Consensus on the Primary Therapy of Early Breast Cancer 2013. *Ann Oncol 2013* **24**: 2206–2223.
49 Schillaci R, Guzman P, Cayrol F, Beguelin W, Diaz Flaque MC, Proietti CJ *et al.* Clinical relevance of ErbB-2/HER2 nuclear expression in breast cancer. *BMC Cancer* 2012; **12**: 74.
50 Wolff AC, Hammond ME, Hicks DG, Dowsett M, McShane LM, Allison KH *et al.* Recommendations for human epidermal growth factor receptor 2 testing in breast cancer: American Society of Clinical Oncology/College of American Pathologists clinical practice guideline update. *J Clin Oncol* 2013; **31**: 3997–4013.
51 Dolled-Filhart M, Camp RL, Kowalski DP, Smith BL, Rimm DL. Tissue microarray analysis of signal transducers and activators of transcription 3 (Stat3) and phospho-Stat3 (Tyr705) in node-negative breast cancer shows nuclear localization is associated with a better prognosis. *Clin Cancer Res* 2003; **9**: 594–600.
52 Rexer BN, Arteaga CL. Intrinsic and acquired resistance to HER2-targeted therapies in HER2 gene-amplified breast cancer: mechanisms and clinical implications. *Crit Rev Oncog* 2012; **17**: 1–16.
53 Arteaga CL, Sliwkowski MX, Osborne CK, Perez EA, Puglisi F, Gianni L. Treatment of HER2-positive breast cancer: current status and future perspectives. *Nat Rev Clin Oncol* 2012; **9**: 16–32.
54 Franklin MC, Carey KD, Vajdos FF, Leahy DJ, de Vos AM, Sliwkowski MX. Insights into ErbB signaling from the structure of the ErbB2-pertuzumab complex. *Cancer Cell* 2004; **5**: 317–328.
55 Browne BC, O'Brien N, Duffy MJ, Crown J, O'Donovan N. HER-2 signaling and inhibition in breast cancer. *Curr Cancer Drug Targets* 2009; **9**: 419–438.
56 Rusnak DW, Lackey K, Affleck K, Wood ER, Alligood KJ, Rhodes N *et al.* The effects of the novel, reversible epidermal growth factor receptor/ErbB-2 tyrosine kinase inhibitor, GW2016, on the growth of human normal and tumor-derived cell lines *in vitro* and *in vivo*. *Mol Cancer Ther* 2001; **1**: 85–94.
57 Kataoka Y, Mukohara T, Shimada H, Saijo N, Hirai M, Minami H. Association between gain-of-function mutations in PIK3CA and resistance to HER2-targeted agents in HER2-amplified breast cancer cell lines. *Ann Oncol* 2010; **21**: 255–262.
58 Scaltriti M, Rojo F, Ocana A, Anido J, Guzman M, Cortes J *et al.* Expression of p95HER2, a truncated form of the HER2 receptor, and response to anti-HER2 therapies in breast cancer. *J Natl Cancer Inst* 2007; **99**: 628–638.

59 Lee RJ, Albanese C, Fu M, D'Amico M, Lin B, Watanabe G *et al*. Cyclin D1 is required for transformation by activated Neu and is induced through an E2F-dependent signaling pathway. *Mol Cell Biol* 2000; **20**: 672–683.

60 Lenferink AE, Busse D, Flanagan WM, Yakes FM, Arteaga CL. ErbB2/neu kinase modulates cellular p27(Kip1) and cyclin D1 through multiple signaling pathways. *Cancer Res* 2001; **61**: 6583–6591.

61 Neve RM, Holbro T, Hynes NE. Distinct roles for phosphoinositide 3-kinase, mitogen-activated protein kinase and p38 MAPK in mediating cell cycle progression of breast cancer cells. *Oncogene* 2002; **21**: 4567–4576.

62 Ostrander JH, Daniel AR, Lofgren K, Kleer CG, Lange CA. Breast tumor kinase (protein tyrosine kinase 6) regulates heregulin-induced activation of ERK5 and p38 MAP kinases in breast cancer cells. *Cancer Res* 2007; **67**: 4199–4209.

63 Koumakpayi IH, Diallo JS, Le Page C, Lessard L, Gleave M, Begin LR *et al*. Expression and nuclear localization of ErbB3 in prostate cancer. *Clin Cancer Res* 2006; **12**: 2730–2737.

64 Leslie K, Lang C, Devgan G, Azare J, Berishaj M, Gerald W *et al*. Cyclin D1 is transcriptionally regulated by and required for transformation by activated signal transducer and activator of transcription 3. *Cancer Res* 2006; **66**: 2544–2552.

65 Andrique L, Fauvin D, El Maassarani M, Colasson H, Vannier B, Seite P. ErbB3 (80 kDa), a nuclear variant of the ErbB3 receptor, binds to the cyclin D1 promoter to activate cell proliferation but is negatively controlled by p14ARF. *Cell Signal* 2012; **24**: 1074–1085.

66 Breuleux M, Schoumacher F, Rehn D, Kung W, Mueller H, Eppenberger U. Heregulins implicated in cellular functions other than receptor activation. *Mol Cancer Res* 2006; **4**: 27–37.

67 Rivas MA, Tkach M, Beguelin W, Proietti CJ, Rosemblit C, Charreau EH *et al*. Transactivation of ErbB-2 induced by tumor necrosis factor alpha promotes NF-kappaB activation and breast cancer cell proliferation. *Breast Cancer Res Treat* 2010; **122**: 111–124.

68 Diaz Flaque MC, Galigniana NM, Beguelin W, Vicario R, Proietti CJ, Russo RC *et al*. Progesterone receptor assembly of a transcriptional complex along with activator protein 1, signal transducer and activator of transcription 3 and ErbB-2 governs breast cancer growth and predicts response to endocrine therapy. *Breast Cancer Res* 2013; **15**: R118.

69 Rivas MA, Venturutti L, Huang YW, Schillaci R, Huang TH, Elizalde PV. Downregulation of the tumor-suppressor miR-16 via progestin-mediated oncogenic signaling contributes to breast cancer development. *Breast Cancer Res* 2012; **14**: R77.

Supplementary Information accompanies this paper on the Oncogene website (http://www.nature.com/onc)